The Effect of the Circadian Rhythm on Load-Induced Bone Formation

Alice Bouchard, Department of Experimental Surgery, McGill University, Montreal

August 2020

A thesis submitted to McGill University in partial fulfillment of the requirement of the degree of Master of Science.

Table of Contents

Abstract

Bone adapts to mechanical loading to meet functional demands via (re)modeling, a process involving bone-forming osteoblasts, bone-resorbing osteoclasts, and mechanosensing osteocytes. It is known that bone turnover markers (bone formation and resorption) measured from serum increase overnight and peak in the early morning, decreasing in the late afternoon. What remains unclear is how circadian rhythms affect adaptive bone (re)modeling in response to mechanical loading. We investigated if time of loading influences gene expression and bone formation to provide insights into whether load-induced bone (re)modeling in mice is regulated by circadian oscillator mechanisms functioning in bone cells.

The left tibia of 10-week-old C57BL/6J female mice underwent 2 weeks of daily (Mon-Fri) dynamic compressive loading (+1200 με at midshaft, 216 cycles/day at 4 Hz, right tibiae as internal nonloaded control). Loading was performed at either Zeitgeber Time (ZT)2 or ZT14. These mice were housed in metabolic cages and in-vivo micro computed tomography (microCT) was performed at day 0, 5, 10, and 15. Images taken on days 5, 10, and 15 were registered onto day 0 images, to quantify changes in bone (re)modeling over time. In separate experiments examining gene expression analysis, mice underwent a single bout of dynamic compressive loading at ZT2 or ZT14. Mice were then euthanized and dissected 1h, 8h or 24h after loading. In addition, sham-loaded mice were placed under anesthesia for the duration of a single loading bout, but not loaded and were euthanized 8h later, resulting in sample collection at ZT 2,6,10,14,18, and 22. Gene expression analysis and serum ELISAs were performed on these mice.

We observed that loading led to significant increases in cortical and trabecular bone mass and microstructure (eg. cortical thickness and trabecular bone volume fraction) as well as increased bone formation in the loaded compared to the control limb. ZT14 loaded mice had significantly greater cortical area fraction (Ct.Ar/Tt.Ar) and cortical thickness (Ct.Th) at the mid-shaft compared to ZT2. The time of loading also affected the response to loading: (Ec.MV/BV, Ec.MTh, Ps.EV/BV, Ps.ES/BS, Ps.ED) at the mid-shaft. We found with qPCR that *Bmal1, Clock*, *Per1* and *Per2* expressed significant circadian rhythms in sham-loaded bone. We observed significant circadian rhythms in bone-specific *Sost* and *Dkk1* as well. Loading at ZT2 led to a significant increase in *Sost* expression after 8h, while loading at ZT14 led to a significant decrease in *Sost* and *Dkk1* after 1h and 24h. Finally, no significant serum rhythms were observed in Sclerostin, P1NP, and TRAP5b.

These data show that the time of loading influences the expression of mechanically-responsive genes, and that these time points result in differences in bone density and microstructure after 2 weeks of loading, as well as varied response to loading at different timepoints. Further studies are required to determine if physical exercise at certain times of day results in enhanced load-induced bone formation in patients.

Résumé

Pour répondre aux demandes fonctionnelles, les os s'adaptent aux charges mécaniques par (re)modelage, un processus qui met à contribution des ostéoblastes, qui stimulent l'ostéoformation, des ostéoclastes, qui stimulent la résorption osseuse, et des ostéocytes mécano-capteurs. Il est établi que les marqueurs du renouvellement osseux (formation et résorption osseuses) mesurés dans le sérum augmentent pendant la nuit et atteignent leur taux maximum à l'aube, puis ils chutent en fin d'après-midi. Ce qui est moins clair, c'est comment les rythmes circadiens affectent le (re)modelage osseux adaptatif en réponse aux charges mécaniques. Nous avons examiné si l'heure de la charge a un effet sur l'expression génétique et l'ostéoformation pour mieux comprendre si le (re)modelage osseux stimulé par une charge chez les souris est régulé par les mécanismes circadiens oscillateurs qui opèrent dans les cellules osseuses.

Le tibia gauche de souris femelles C57BL/6J âgée de 10 semaines a été soumis quotidiennement (du lundi au vendredi) pendant 2 semaines à une charge compressive dynamique (+1200 με au milieu du corps de l'os, 216 cycles/jour à 4 Hz, le tibia droit servant de contrôle interne non chargé). La charge a été appliquée à l'une ou l'autre des heures de référence Zeitgeber (ZT)2 ou ZT14. Ces souris étaient hébergées dans des cages métaboliques et une micro-tomographie (microCT) *in vivo* a été effectuée les jours 0, 5, 10 et 15. Les images captées les jours 5, 10 et 15 ont été enregistrées par-dessus les images du jour 0 afin de quantifier les changements dans le (re)modelage osseux en fonction du temps. Dans des expériences distinctes examinant l'expression génétique, les souris ont été soumises à une seule session de charge compressive dynamique à ZT2 ou ZT14. Les souris ont ensuite été euthanasiées et disséquées 1h, 8h ou 24h après la charge. De plus, des souris faussement chargées ont été anesthésiées pendant la durée

d'une session de charge, sans charge réelle, puis euthanasiées 8h plus tard. L'analyse de l'expression génétique et un essai ELISA sérologique ont été effectués sur ces souris.

Nous avons observé que la charge a entraîné une augmentation significative de la masse et des microstructures osseuses corticales et trabéculaires (par ex. épaisseur corticale et fraction volumique de l'os trabéculaire) de même qu'une ostéoformation accrue dans les membres chargés comparativement aux membres de contrôle. Les souris chargées à ZT14 présentaient une augmentation nettement plus grande de l'aire corticale (Ct.Ar/Tt.Ar) et de l'épaisseur corticale (Ct.Th) au milieu du corps de l'os, comparativement à ZT2. L'heure de la charge affectait également la réponse à la charge : (Ec.MV/BV, Ec.MTh, Ps.EV/BV, Ps.ES/BS, Ps.ED) au milieu du corps de l'os. Nous avons observé avec qPCR que *Bmal1, Clock*, *Per1* et *Per2* manifestaient des rythmes circadiens significatifs dans les os faussement chargés. Nous avons aussi observé des rythmes circadiens significatifs au niveau de *Sost* et *Dkk1,* des gènes spécifiques au tissu osseux. Effectuée à ZT2, la charge a entraîné une augmentation significative de l'expression de *Sost* après 8h, tandis qu'à ZT14, la charge a entraîné une baisse significative de *Sost* et *Dkk1* après 1h et 24h. Finalement, aucun rythme sérologique significatif n'a été observé au niveau de Sclerostin*,* P1NP et TRAP5b.

Ces données montrent que l'heure de la charge influence l'expression des gènes mécaniquement sensibles, et que ces points temporels entraînent des différences dans la densité et les microstructures osseuses après 2 semaines de charge ainsi qu'une réponse variable à la charge selon le moment de la journée. D'autres études seront requises pour déterminer si l'exercice physique pratiqué à certains moments de la journée stimule davantage la formation osseuse induite par une charge chez les patients.

Acknowledgements

I would first like to thank my supervisor and mentor, Dr. Bettina Willie. Thank you for giving me the opportunity to conduct this research and learn numerous techniques. Thank you for guiding me throughout this process and helping me to improve my scientific writing. Thank you for supporting me as I pursue my dreams, and for being so understanding when I was not sure what those dreams were. You have been a tremendous role model and I am so grateful I had the opportunity to work for you.

I would like to thank Maximilian Rummler for first welcoming me in the lab, for bearing with all of my questions, for teaching me new techniques, and for showing me how to turn on a computer. You have been such a helpful lab mate and friend, and I could not have gotten this far without you.

Je veux remercier Catherine Julien pour toute son aide. Tu m'as aidée à tous moments, pendant nos expériences, en écrivant notre article, en répondant à mes questions, et en m'aidant à rester calme quand j'ai fait des erreurs.

I also want to thank Elizabeth Zimmermann for being a great role model and a tremendous help in the lab. You never hesitated to help me when I got stuck, help me calm down and think about a problem, and always being someone I could talk to about anything.

I would like to thank each and every one in my lab – David Bertrand, Kyle Kavaseri, Mahdi Hosseinitabatabaei, Beatrice Steyn, Isabella Vitienes, Aren Bezdjian, Chrisanne Dsouza, Marie-Helene Gaumond -- from helping me with experiments, to making me laugh in the cafeteria, you have all been the highlight of my master's. Special thanks to Mahdi and Isabella – I don't think

anyone else will ever understand that Saskatoon trip, or have to put up with my hyperactivity when I am exhausted.

I owe a huge debt of gratitude to each of my friends. You have been my rocks, whether it was through skiing weekends, dinner parties, or simply your words of encouragement. Thank you!

Thank you to Harriet Yan. You have put up with me at my best and my worst, you have helped me edit posters and presentations, supported me no matter what, and been a great friend. I can't express how much you have helped me.

Thank you to Hannah Burr. Your support throughout this process has been endless and I would not be at this point without you.

Finalement, un petit mot pour ma famille. Votre patience, votre réconfort et votre support n'ont pas de limite. Vous m'inspirez chaque jour et je ne crois pas que j'aurais terminé cette maîtrise sans votre aide. À travers la Covid-19 et toutes mes incertitudes, vous avez été constants et je vous remercie de toute mon cœur.

Contribution of Authors

Chapter 1 (Background & Rationale), Chapter 3 (Extended Discussion), Chapter 4 (Conclusion & Summary) were written by Alice Bouchard and revised by Dr. Bettina Willie.

Chapter 2 – *Bone adaptation to mechanical loading in mice is affected by circadian rhythm*, currently in submission.

A. Bouchard – performed all tissue-level experiments and analysis, performed all statistical analyses, drafted manuscript.

C. Dsouza – conducted qPCR, revised manuscript.

C. Julien – conducted gene-level experiments and analysis, revised manuscript.

M. Rummler – conducted gene-level experiments, performed activity data analysis, revised manuscript.

M.H. Gaumond – conducted qPCR, conducted ELISAs, revised manuscript.

B. Willie – Study design, conducted gene-level experiments, supervisory support, funding procurement, revised manuscript.

In addition to the manuscript presented in this thesis, I am also a co-author on several other projects described below.

1) Rummler M, Ziouti F, **Bouchard A**, Brandl A, Duda GN, Bogen B, Beilhack A, Lynch M, Jundt F, Willie BM. Mechanical stimulation rescues bone loss and exerts cell-extrinsic anti-tumor effects in the MOPC315.BM.Luc model of myeloma bone disease. Acta Biomater. 2020 Oct 29:S1742-7061(20)30639-5.

Performed calcein histomorphometry imaging and analysis.

2) Bezdjian A, **Bouchard A**, Rummler M, Zimmermann E, Daniel S, Willie BM. Temporal Skull Bone Characterisation With Respect to Bone-Anchored Hearing Implant Placement; a Human Cadaveric Bone Model; *TBD*; In preparation.

   Performed microCT imaging.

3) Vitienes I, **Bouchard A**, Hosseinitabatabaei S., Julien C, Komarova S, Widowski T, Willie BM. Examining the effect of chicken strain on the daily mechanical strain stimuli during background activity in pullets; *TBD*; In preparation.

   Assisted and performed strain-gauging surgery and background strain gauging experiments.

4) Ross E, Vitienes I, Graceffa G, **Bouchard A**, Willie BM, Widowski T. The effect of housing, chicken strain, and age of pullets on bone mass and microarchitecture; *TBD*; In preparation.

   Performed analysis of microCT images.

List of Figures

List of Tables

Abbreviations

***Axin2* –** Axin related protein 2

BFR – Bone formation rate

***Bglap* –** Bone gamma-carboxyglutamate protein

BMAL1 (*Bmal1)* – Bone muscle ARNT-like 1

BMD – Bone mineral density

BMU – Basic multicellular unit

CLOCK (*Clock)* – Circadian locomotor output cycles kaput

Ct – Cortical

Ct.Ar – Cortical area

Ct.Ar/Tt.Ar. – Cortical area fraction

Ct.Th – Cortical thickness

***Ctsk* –** Cathepsin k

CTX – Carboxy-terminal collagen crosslinks

DKK1 (*Dkk1)* – Dickkopf-related protein 1

dLS – Double labeled surface

Ec – Endocortical

ED – Eroding depth

ELISA – Enzyme Linked Immunosorbent Assay

ES/BS – Eroding surface

EV/BV – Eroding volume

FGF-23 – Fibroblast growth factor 23

***Lef1* –** Lymphoid enhancer binding factor 1

Ma.Ar – Marrow area

MAR – Mineral apposition rate

microCT (μCT) – Micro computed tomography

mRNA – Messenger ribonucleic acid

MS/BS – Mineralizing surface

MTh – Mineralizing thickness

MV/BV – Mineralizing volume

P1NP – Procollagen 1 Intact N-terminal Propeptide

PER1 (*Per1)* – Period 1

PER2 (*Per2)* – Period 2

Ps – Periosteal

PTH – Parathyroid hormone

qPCR – Quantative polymerase chain reaction

***Runx2* –** Runt-related transcription factor 2

Scl-Ab – Sclerostin neutralizing antibody

SCN – Suprachiasmatic nucleus

sLS – Single labeled surface

***Sost* –** Sclerostin

***Sp7* –** Osterix

Tb – Trabecular

Trap5b – Tartrate-resistant Acid Phosphatase 5b

Wnt – Wingless related integration site

ZT – Zeitgeber Time

Chapter 1: Background and Rationale

1.1 Bone

Bone is an extraordinary tissue responsible for various functions of the body, including providing an organism's skeletal structure, protecting the thoracic cavity and bone marrow, providing the body with a reservoir of essential minerals, and secreting chemokines, cytokines, and growth factors (Su et al., 2019). Bone is organized in a hierarchical fashion, lending the tissue its structure and function (Burr, 2019). At bone's most basic form, it is made up of collagen fibrils, that are interspersed with minerals such as phosphate and calcium (Burr, 2019). These collagen fibers are then grouped into osteons, a canal surrounded by lamella in cortical bone, or trabeculae, also made up of lamella in trabecular bone (Burr, 2019).

Despite its structural complexity, bone is not a static tissue. Bone, like most tissues in the body, is involved in restructuring (modeling) and regular turnover, removing older bone to replace it with new bone (remodeling) (Robling & Turner, 2009). Bone remodeling is mediated by bone forming osteoblasts, bone resorbing osteoclasts, and mechanosensing osteocytes embedded within the bone (Su et al., 2019). This process is performed by basic multicellular units (BMUs), composed of osteoclasts and osteoblasts (A. Michael Parfitt, 2013). While modeling is not coordinated, remodeling involves spatial and temporal coordination between osteoblasts and osteoclasts. These BMUs will operate in specific locations, bringing osteoclasts to resorb bone, and osteoblasts directly afterwards to this same area to replace the bone that has been lost. In humans, this process can occur both within the cortical bone (intracortical remodeling via the BMU) and on the bone surfaces (A. M. Parfitt, 1994). Mice also remodel on the bone's surface but lack osteons. Thus intracortical remodeling does not normally occur in mice (Jilka, 2013;

Piemontese et al., 2017). In both species however, remodeling leads to the turnover of the entire skeleton, helping to limit bone age, heal microcracks, retain mechanical competence, and maintain calcium homeostasis (A. Michael Parfitt, 2013).

In addition to (re)modeling, bone actively responds to its mechanical environment to meet the requirements of day-to-day physical activity (J. Wolff, 1892). This concept has been generally understood since Galileo's time, and more specifically stated in Wolff's law in 1892 (Willie, Zimmermann, Vitienes, Main, & Komarova, 2020). Wolff stated that:

> *Every change in the form and function of bone or of their function alone is followed by certain definite changes in their internal architecture, and equally definite alteration in their external conformation, in accordance with mathematical laws (Frost, 1994).*

Despite this assertion, however, he was not able to state how this process occurs (Frost, 1994). Much later in 1987 it was proposed by Harold Frost that bone acts as a mechanostat (Frost, 1987). Essentially, bone tissue has a "setpoint" of strain, above which, bone formation will be triggered. This formation will lead to more bone, to protect the structure from damage associated with higher strains (Frost, 1987). The increased amount of tissue will raise the "setpoint" such that the previous mechanical load may no longer be sufficient to trigger bone formation (Frost, 1987). Lower strains will cause the opposite result – bone will be resorbed if it is not needed (Frost, 1987). Clinically, this phenomenon has been demonstrated in several papers which show that the playing arm of tennis players, the loaded arm, exhibits significantly more bone than the nonloaded arm (Haapasalo et al., 2000; Jones, Priest, Hayes, Tichenor, & Nagel, 1977; Kontulainen, Sievanen, Kannus, Pasanen, & Vuori, 2003) while bones that are unloaded, for instance through microgravity experienced in spaceflight, exhibit bone loss (Lang et al., 2004).

Although the evolutionary rationale behind bone resorption during unloading is less clear, adaptive bone formation has proven to be beneficial in many contexts.

Mechanical loading has been shown to improve bone mineralization in children (Ducher, Tournaire, Meddahi-Pelle, Benhamou, & Courteix, 2006), maintain bone health into adulthood, and protect against age-related bone loss (Beck & Snow, 2003; Engelke et al., 2006; Kohrt, Snead, Slatopolsky, & Birge, 1995; Korpelainen, Keinanen-Kiukaanniemi, Heikkinen, Vaananen, & Korpelainen, 2006). The global population of persons with osteoporosis continues to rise, affecting countless people worldwide (Hernlund et al., 2013). In the United States alone, an estimated 54 million people are affected by osteoporosis or bone fragility ("National Osteoporosis Foundation,"). Beyond simply affecting the health and well-being of these individuals, the economic burden of this disease continues to increase (Svedbom et al., 2013). Current treatments for osteoporosis include lifestyle modifications, such as smoking cessation, nutritional supplements, and physical activity, pharmacological agents such as bisphosphonates and estrogen replacement that work as antiresorptive agents, and some anabolic pharmacological agents, like sclerostin neutralizing antibody (Tabatabaei-Malazy, Salari, Khashayar, & Larijani, 2017). Each treatment comes with its own downsides, for instance very high cost or low patient compliance, thus there does not seem to be a perfect method to combat osteoporosis (Tabatabaei-Malazy et al., 2017). Combined approaches, for instance combining anabolic or anti-catabolic drugs with physical activity, may act synergistically, and might even reduce drug dosage (Braith et al., 2007; Leblanc et al., 2013). Therefore, it is essential to understand the effects of mechanical loading in a variety of situations. One aspect previously overlooked may involve fighting osteoporosis through mechanical loading targeted specifically when load-induced bone formation is most effective.

1.2 Mechanotransduction

Bones sense mechanical loads through a process called mechanotransduction. Osteocytes embedded within the bone sit within lacunae (Baud, 1962). They possess processes that are long finger-like projections, dendrites, that extend through the canaliculi (Baud, 1962). The lacunar-canilicular network that the osteocytes reside in are filled with fluid (Dallas, Prideaux, & Bonewald, 2013). As an organism exerts mechanical force on their bones, through movement, this fluid will move, resulting in fluid-flow in the lacunar-canilicular network that creates shear-stress on osteocytes (Yavropoulou & Yovos, 2016). After sensing shear stress, osteocytes use downstream signaling pathways in order to communicate with osteoblasts and osteoclasts to trigger bone formation (L. F. Bonewald & Johnson, 2008). Perhaps the most important of these signaling pathways is the wnt/B-catenin pathway that results in bone formation in response to loading (L. F. Bonewald & Johnson, 2008). It has been shown that mechanical loading leads to a down-regulation in sclerostin expression (Robling et al., 2008). Sclerostin, a wnt signaling inhibitor, has become increasingly important in the bone field. Sclerostin is a protein secreted by mature osteocytes, which acts to inhibit the wnt-signaling pathway by binding to LRP5/6 and blocking downstream signaling, thereby inhibiting bone formation (Delgado-Calle, Sato, & Bellido, 2017). Sclerostin has gained recognition as a very important protein through conditions such as sclerosteosis (Brunkow et al., 2001). In this disease, sclerostin (*Sost*) is not expressed, and patients display vast overgrowths of bone (Brunkow et al., 2001). For these patients, the bone overgrowth is detrimental as it increases intracranial pressure, entraps the 7^{th} and 8^{th} cranial nerves, and leads to sudden death (Brunkow et al., 2001). However, for patients lacking bone, perhaps using this knowledge of *Sost*'s role as a wnt signaling inhibitor can be beneficial. As a result, sclerostin-neutralizing antibodies have become a promising anabolic treatment for bone

fragility conditions since reducing *Sost* levels may promote bone formation (Baron & Hesse, 2012). In addition to the importance of *Sost* in pathologies, *Sost* is believed to play a key role in load-induced bone formation. It has been previously reported that *Sost* mRNA levels in the bone are reduced upon loading in the ulnae of mice (Robling et al., 2008). Thus, the downregulation of *Sost* has been proposed as a key to how mechanical-load induced bone formation occurs.

1.3 Circadian Rhythm

An aspect of load-induced bone formation that has been as of yet overlooked is how the circadian rhythm impacts this process. Circadian rhythms have increasingly been implicated in the natural function of various body systems (Dibner, Schibler, & Albrecht, 2010). At its core, the circadian rhythm is a negative feedback molecular loop (Sangoram et al., 1998; Sato et al., 2006). Transcription factors CLOCK and BMAL1 translocate to the nucleus where they promote the transcription of *Per* and *Cry* genes (Reppert & Weaver, 2002). Following translation, PER and CRY proteins dimerize and are phosphorylated, allowing them to move to the nucleus, where they block the interaction of BMAL1 and CLOCK (Reppert & Weaver, 2002). This feedback loop is a conserved mechanism, present in nearly all cells in the body (Dibner et al., 2010). In addition to their roles in this molecular loop, BMAL1, CLOCK, PER, CRY, and others are transcription factors for many other genes, resulting in the rhythmic expression of many tissue-specific genes (Duguay & Cermakian, 2009). These genes, not rhythmic on their own, are called clock-controlled genes.

Circadian rhythms have been well characterized in many tissues, such as the liver, heart, and digestive system (Dibner et al., 2010). Recently, it has become increasingly clear that bone displays a circadian rhythm. Some bone turnover markers have been found to oscillate in human

serum and plasma (Greenspan, Dresner-Pollak, Parker, London, & Ferguson, 1997; C. Swanson et al., 2017; van der Spoel et al., 2019). CTX, osteocalcin, and FGF-23 have been shown consistently to have a diurnal rhythm which increases overnight, peaks early in the morning, and displays a nadir in the late afternoon (Qvist, Christgau, Pedersen, Schlemmer, & Christiansen, 2002; Redmond et al., 2016; C. Swanson et al., 2017). P1NP rhythmicity on the other hand, has only been observed in some instances (Greenspan et al., 1997; Luchavova et al., 2011; Redmond et al., 2016; C. Swanson et al., 2017; van der Spoel et al., 2019). There have also been contradictory findings reported for serum sclerostin. One group observed a diurnal rhythm in serum sclerostin in 21-32 year-old healthy men (Santosh HS, 2013), while another study did not observe a discernable rhythm in 20-65 year-old healthy men (C. Swanson et al., 2017). The contradictory results may be due to a variety of environmental factors and currently available commercial assays may require further investigation before they can be used routinely in the clinic (Clarke & Drake, 2013). In addition to rhythmic bone turnover markers, osteoblasts and osteoclasts express core circadian rhythm proteins (Fujihara, Kondo, Noguchi, & Togari, 2014; Samsa, Vasanji, Midura, & Kondratov, 2016). Fujihara et al. demonstrated that osteoclasts express both *Per2* and *Bmal1* mRNA, while Samsa et al. illustrated that disrupted *Bmal1* expression leads to disrupted osteoblast differentiation and overall reduced numbers of osteoblasts and osteoclasts (Fujihara et al., 2014; Samsa et al., 2016). Comparatively little is known regarding the circadian rhythm of osteocytes – one group only has demonstrated *Bmal1* expression in osteocytes through immunohistochemistry (Takarada et al., 2017).

To coordinate the various rhythms of peripheral clocks in the body, and ensure an organism appropriately responds to its external environment, various cues can synchronize the circadian rhythm. Known as zeitgebers, or time givers, cues such as light, exercise, and food have the

ability to synchronize behavior and bodily functions to the environment (Dibner et al., 2010). The most powerful of these stimuli, light, is sensed by the retina and signals are sent through the retinohypothalamic tract to the suprachiasmatic nucleus, the central circadian clock in the brain (Klein, Moore, & Reppert, 1991). From here, the SCN synchronizes peripheral clocks in each tissue through hormonal, nervous system, or other cues. Interestingly in some peripheral tissues, zeitgebers like feeding appear to have greater importance than that of light (Dibner et al., 2010). It is as of yet unknown whether bone may preferentially entrain to signals such as activity or feeding. However, since exercise has been shown to entrain the peripheral clock in muscle (G. Wolff & Esser, 2012), and the crosstalk between bone and muscle is increasingly understood to play an essential role (L. Bonewald, 2019), it is likely that activity plays some role in entraining the bone's peripheral clock.

Although the anabolic effect of mechanical loading on bone is well established, its intersection with the circadian rhythm has not yet been defined, and thus the therapeutic benefit of mechanical loading as a chronotherapy (providing a treatment at a specific time of day) has not yet been studied. However, some studies in orthodontics have investigated the impact of applying mechanical force to the teeth of rats either during the active phase or the resting phase (Igarashi, Miyoshi, Shinoda, Saeki, & Mitani, 1998; Miyoshi, Igarashi, Saeki, Shinoda, & Mitani, 2001; Oudet, Petrovic, & Stutzmann, 1984; Yamada et al., 2002). These experiments suggest that applying mechanical force to the teeth or mandible strictly during the resting phase leads to greater movement than during the active phase. Other groups have investigated similar ideas in muscle, determining that the muscle has its own circadian rhythm, and that exercise has the ability to phase shift the muscle's circadian rhythm (G. Wolff & Esser, 2012). Taken in

concert, these studies suggest that zeitgeber time may play a crucial role in bone formation, bone-muscle crosstalk, and mechanical load induced bone formation.

1.4 Hypothesis and Aims

We hypothesized that the central circadian rhythm controls the peripheral clock in bone, optimizing its response to mechanical loading at various times of day such that mechanical loading during the day would result in more or less bone formation than loading during the resting phase. To investigate this, we designed an experiment consisting of two aims: first, to determine if the zeitgeber time of loading influences the adaptive bone formation response and second, to determine if the zeitgeber time of loading affects osteoblast and osteocyte gene expression. This study consisted of applying a mechanical load to the left tibia of 10-week-old female C57Bl/6J mice, either during the day at ZT2 (8am) or during the night at ZT14 (8pm). These mice were loaded once per day for 2 weeks, and their tibiae were scanned every 5 days for the duration of the experiment. In addition, we mechanically loaded female 10-week-old C57Bl/6J mice once at various points during the day and mice were dissected 1, 8, or 24 hours later in order to study gene expression in the tibiae, bone marrow, and serum. The results of these experiments are detailed in the following chapter "*Bone adaptation to mechanical loading in mice is affected by circadian rhythm*" a manuscript which has been submitted for peer review.

Chapter 2: *Bone adaptation to mechanical loading in mice is affected by circadian rhythm*

Bone adaptation to mechanical loading in mice is affected by circadian rhythm

Alice L. Bouchard[1], Chrisanne Dsouza[1], Catherine Julien[1], Maximillian Rummler[1], Marie-Hélène Gaumond[1], Bettina M. Willie[1] *

[1]*McGill University, Research Centre, Shriners Hospital for Children-Canada, Department of Pediatric Surgery, McGill University, Montreal, Canada*

*Bettina M. Willie

Shriners Hospitals for Children-Canada

1003 Decarie Blvd

Montreal, H4A 0A9, Canada

Phone: +1 514-282-7156

Email: bwillie@shriners.mcgill.ca

Keywords

Bone, mechanobiology, chronobiology, mechanical loading, sclerostin

Author Contributions

Study design: BW. Data acquisition: AB, CD, CJ, MHG. Data analysis: AB, CD, MR, CJ, BW. Data interpretation: All authors. Drafting manuscript: AB, BW. Revising manuscript content: All authors. Approving final version of manuscript: All authors. BW takes responsibility for the integrity of the data.

Abstract

Physical forces are critical for successful function of many organs including bone. Interestingly, the timing of exercise during the day has been shown to alter physiology and gene expression in many organs due to circadian rhythms. Circadian clocks in tissues such as bone have circadian genes that target tissue-specific genes (clock-controlled genes), resulting in tissue-specific rhythmic gene expression. We hypothesized that the adaptive response of bone to mechanical loading is regulated by circadian rhythms. We performed controlled *in vivo* tibial loading in mice either in the morning, zeitgeber time (ZT2, resting phase) or evening (ZT14, active phase). The tissue level mechanoresponse after two weeks of loading was quantified in terms of formed and resorbed bone volume on the endocortical and periosteal surfaces. We demonstrated that loading at ZT14 resulted in a greater endocortical bone formation response compared to mice loaded at ZT2. In a separate experiment, mice were subjected to a single bout of *in vivo* loading either ZT2 or ZT14 and then were sacrificed after 1, 8, or 24 hours. In addition, sham-loaded mice were anesthetized for the duration of one loading cycle, and dissected 8 hours later, resulting in 6 different timepoints throughout the day. Sham-loaded mice displayed diurnal expression of core clock genes and osteocyte-specific genes, such as the *Wnt*-signaling inhibitors *Sost* and *Dkk1,* suggesting they are clock controlled genes. Loading at ZT2 resulted in *Sost* upregulation, while loading at ZT14 resulted in downregulated *Sost* and *Dkk1* expression. The time-of-day specific increases in adaptive bone formation coincident with decreased *Sost* and *Dkk1* expression suggest that circadian clocks are key determinants in the mechanoresponse of bone.

Significance Statement

Osteocytes sense mechanical stimuli and signal to osteoblasts and osteoclasts to form and resorb bone, respectively. Bone cells express peripheral clock genes. We demonstrate that the time of day at which loading is administered influenced the mechanoresponse in a site-specific manner. Loading in the evening (active phase) compared to the morning (rest phase) resulted in greater endocortical bone formation, coincident with differential *Sost* expression. This was accomplished by measuring the amount of newly formed bone at endocortical and periosteal surfaces and gene expression in response to controlled tibial loading of mice. The established relationship between increased bone formation and differential *Sost* expression based on time-of-day in mice implies the possibility for exercise-based therapies to enhance bone mass in patients.

Introduction

Physical forces are vital for successful function of musculoskeletal, urinary, respiratory, and other organ systems. Mechanical loading is an important cue for bone, leading to bone adaptation, whereby bone is formed or resorbed to meet the local changing mechanical environment (Willie et al., 2020). Bone mass is strongly affected by the mechanical environment, as emphasized by bone loss in paralyzed or bedridden patients. Bone cells are critical executors of bone adaptation; osteocytes are the mechano-strain sensors in the bone that coordinate bone formation by osteoblasts and resorption by osteoclasts. Mechanical loading modulates cell numbers and activity, adjusting the material properties (strength, elasticity, toughness) and the bone's size and shape, to withstand the applied forces(Pivonka, 2018).

Exercise is potentially the most efficient and cost-effective intervention to improve bone health. While it is clear that physical activity can enhance bone mass (Jones et al., 1977), it remains unknown if the time at which exercise is performed can alter adaptive bone formation or resorption in humans. The timing of exercise during the day has been shown to alter physiology and gene expression in the adrenals, liver, and heart due to circadian rhythms (Schroeder et al., 2012). Studies in muscles show the time of day that exercise is performed can lead to phase shifting of peripheral clocks(G. Wolff & Esser, 2012), which has implications for bone, due to bone-muscle crosstalk (L. Bonewald, 2019). Time of day at which forces were applied to teeth in rats led to higher alveolar bone formation (Miyoshi et al., 2001; Oudet et al., 1984). These studies suggest that the time of day of mechanical stimuli may affect the periodontal tissue remodeling, however the loading was not well controlled and there were large variations reported in tooth movement and tissue response in the studies.

The mammalian circadian system includes a central clock located in the suprachiasmatic nucleus (SCN) in the hypothalamus (M. Hastings, 1998; M. H. Hastings & Herzog, 2004), which at the molecular level involves a highly conserved negative feedback loop. Brain and muscle ARNT-like 1 (BMAL1) and circadian locomotor output cycles kaput (CLOCK) are transcription factors that work together and bind to the e-box in the promoter region of *Per* and *Cry* genes, promoting their transcription and translation (Asher & Schibler, 2011; Reppert & Weaver, 2002). PER and CRY proteins then dimerize and inhibit the actions of CLOCK and BMAL1 (Reppert & Weaver, 2002). This cycle takes approximately 24 hours to complete and the central clock can be synchronized by various external signals, also called zeitgebers, such as light, feeding, and exercise (Dibner et al., 2010). The SCN synchronizes the peripheral clocks via neuronal or hormonal mechanisms. Studies have shown communication between the central clock and bone cells. The SCN and bone-forming osteoblasts communicate via the sympathetic nervous system and glucocorticoids (Hirai, Tanaka, & Togari, 2014; Komoto, Kondo, Fukuta, & Togari, 2012). Glucocorticoids are also implicated in the synchronization of osteoclasts, bone resorbing cells, by the SCN (Fujihara et al., 2014). It remains unclear if and how the SCN communicates with osteocytes, which are the cells that sense mechanical cues and translate these into molecular signals of resorption and formation (Inaoka et al., 1995; Skerry, Bitensky, Chayen, & Lanyon, 1989), thereby orchestrating bone (re)modeling (modeling and remodeling) (A. Michael Parfitt, 2013).

In addition to synchronization from the central clock, peripheral tissue clocks may respond to certain zeitgebers independently of the SCN (Dibner et al., 2010; Takahashi, Hong, Ko, & McDearmon, 2008; Yoo et al., 2004). Many tissues, including bone, harbor peripheral clocks.

Peripheral clocks have circadian genes that target tissue-specific genes, resulting in tissue-specific rhythmic gene expression(Reppert & Weaver, 2002). Several studies have shown that osteoblasts and osteoclasts express rhythmic clock genes (Fu, Patel, Bradley, Wagner, & Karsenty, 2005; Fujihara et al., 2014), while only one study has shown the expression of BMAL1 in osteocytes (Takarada et al., 2017). Osteoblast-specific *Bmal1*$^{-/-}$ mice have a low BMD phenotype due to higher levels of bone resorption, while osteoclast-specific conditional *Bmal1*$^{-/-}$ mice have a high BMD phenotype due to decreased bone resorption (Takarada et al., 2017; Xu et al., 2016). McElderry et al. reported that bone mineral deposition in murine calvarial organ cultures showed a 24-hr periodicity and could be correlated to clock gene expression (McElderry et al., 2013). The bone resorption marker CTX, bone mineralization marker produced by osteoblasts, osteocalcin, and the regulator of phosphate metabolism FGF-23 secreted by osteocytes, measured from human serum have been shown consistently to have a diurnal rhythm (Qvist et al., 2002; Redmond et al., 2016; C. Swanson et al., 2017). All three of these proteins increase overnight, peak in the early morning, and display a nadir in the late afternoon. In contrast, there have been conflicting reports of P1NP rhythmicity, a common marker for formation (Greenspan et al., 1997; Luchavova et al., 2011; Redmond et al., 2016; C. Swanson et al., 2017; van der Spoel et al., 2019). It was suggested that osteocytes may direct the rhythmicity of other bone turnover markers, however, there have been contradictory findings reported for serum sclerostin. One group observed a diurnal rhythm in serum sclerostin in 21-32 year-old healthy men (Santosh HS, 2013), while another study did not observe a discernable rhythm for serum sclerostin from 20-65 year-old healthy men (C. Swanson et al., 2017). It is assumed that bone turnover marker rhythms are controlled by endogenous circadian cues to regulate bone metabolism, but the rhythms may also be influenced by exogenous cues, like

behavioral or environmental changes. Swanson et al. (C. M. Swanson et al., 2017) recently showed that sleep restriction with concurrent circadian disruption led to a rapid decline in P1NP. They did not examine long-term effects on bone mass, but these data highlight the role of circadian rhythms in bone homeostasis.

In our study we aimed to determine if there are tissue-level and gene-level change in bone's response to mechanical loading at different times of day using a controlled murine tibial loading model (Main et al., 2020). We hypothesized that 1) time of day that *in vivo* loading is administered (the zeitgeber time) affects the bone formation and resorption response and that 2) bone (re)modeling in response to mechanical loading is regulated at the molecular level by the circadian rhythms through peripheral clocks in osteocytes. To test the first hypothesis, we applied *in vivo* dynamic axial compressive loading to the tibiae of young female C57BL/6J mice over a two-week period during which time we also performed *in vivo* microCT imaging every five days (Fig. 1). *In vivo* loading was performed on the left limb either in the morning, zeitgeber time 2 (ZT 2) or evening (ZT 14), while the right limb was not loaded (n=10 mice/ZT). The response to a controlled mechanical loading was quantified in terms of newly formed and resorbed cortical bone on both the inner endocortical and the outer periosteal surfaces of the tibiae using 3D registered micro-CT based time-lapse *in vivo* morphometry following our established methods (39). We examined trabecular bone in the metaphysis of the proximal tibia. Conventional (unregistered) microCT analysis and histomorphometry were also performed on both bone compartments. All mice were housed for the entire experiment in metabolic cages so that their background activity could be measured starting 5 days prior to and 15 days following the onset of the *in vivo* loading.

To test the second hypothesis, the left tibia of young female C57BL/6J mice underwent a single loading session at ZT2 or ZT14 and then were sacrificed 1, 8, or 24 hours post-loading (n=6/time point) to measure early, middle, and late responding genes using qPCR. Additional mice were sham loaded (anesthetized for the same duration as loaded mice, ~5 mins) at ZT2, 6, 10, 14, 18, and 22 (n=6/time point) and were euthanized 8-hours later to measure gene and serum protein expression using qPCR and ELISA, respectively.

Results

Loading led to a robust bone formation response

3D registered micro-CT based time-lapse morphometry parameters, which incorporated 3D image registration to analyze the exact volume of interest at the mid-diaphysis on day 0 and day 15 revealed a robust diaphyseal endocortical bone formation response to loading evident by significantly increased volume (Ec.MV/$BV_{day0-15}$:185%) surface area (Ec.MS/$BS_{day0-15}$:66%) and thickness (Ec.$MTh_{day0-15}$:51%) of newly mineralized endocortical (Ec.) bone over the 15 day scanning interval in the loaded compared to nonloaded control limbs. On the periosteal surface, loading led to a significant increase in Ps.MV/$BV_{day0-15}$ (115%, loaded vs. control limb) (Fig. 2; Table 1).

On day 15, diaphyseal cortical unregistered microCT parameters (Ct.Ar: 133%, Ct.Ar/Tt.Ar: 421%, Ct.Th: 377%) were significantly greater in loaded limbs compared to control limbs. However, unexpectedly, we observed handedness in Imax and Ct.Ar, meaning significant differences were observed between the right and left tibiae at baseline (day 0, the onset of loading). Since we are using the right limb as a nonloaded internal control, which is the

convention in the field (Main et al., 2020), we therefore also analyzed the change from baseline (Δ=day15-day0) for the conventional microCT data. The change from baseline using unregistered images from day 15 and day 0 for the control limb was compared to the change from baseline using unregistered images from day 15 and day 0 for the loaded limb. Similar to our initial analysis, we observed a significant increase in ΔCt.Ar , ΔCt.Ar/Tt.Ar, and ΔCt.Th and a significant decrease in ΔMa.Ar in the loaded compared to the control limb (Supplemental fig. 1). Two-dimensional conventional histomorphometry confirmed loading-induced bone formation effects in one parameter measured (loaded vs control limb) on the endocortical surface (Ec.sLS/BS) and one parameter measured on the periosteal surface (Ps.MS/BS). However, nearly all control limb images lacked periosteal double labeling, thus periosteal histomorphometry analysis was limited (Supplemental Fig. 2; Supplemental Table 1).

At the metaphyseal region, we also observed a robust load-induced cortical and trabecular bone formation response to loading (Figure 3, Table 1, Supplementary Results).

Time of day at which loading is administered influenced bone formation response to loading in a site-specific manner

At the midshaft region, we observed that mice loaded at ZT14 exhibited a greater cortical bone formation response than mice loaded at ZT2. MicroCT-based 3D registered time-lapse morphometry at the tibial midshaft confirmed a greater diaphyseal cortical bone formation response to loading in the ZT14 compared to ZT2 mice (Fig. 2). In mice loaded at ZT14, the volume of newly mineralized endocortical bone over the fifteen days, normalized to the bone volume at day 0, $Ec.MV/BV_{day0\text{-}15}$ was greater (276% increase in loaded vs control limb)

compared to mice loaded at ZT2 (72% increase). The surface area of newly mineralized endocortical bone, Ec.MS/BS $_{day0-15}$ had a similar trend with a 292% increase in ZT14 mice (loaded vs control) compared to a 95% increase in ZT2 mice (loaded vs control) (p=0.07) (Fig. 2; Table 1). The thickness of the newly mineralized endocortical bone, Ec.MTh$_{day0-15}$ also displayed a similar trend with a 71% increase in ZT14 mice (loaded vs control) compared to 26% in ZT2 mice in (loaded vs control) (p=0.06) (Fig. 2; Table 1). Endocortical resorption parameters did not exhibit any significant differences between ZT14 and ZT2 mice.

On the periosteal surface of the midshaft, we did not see an effect of zeitgeber time on bone formation parameters, but mice loaded at ZT14 had a greater resorption response (Ps.EV/BV$_{day0-15}$, Ps.ES/BS $_{day0-15}$, Ps.ED$_{day0-15}$) to loading than mice loaded at ZT2 (Fig. 2; Table 1).

Conventional microCT analysis of day 15 images revealed that the loaded vs control limb cortical area fraction (Ct.Ar/Tt.Ar) was significantly greater in ZT14 mice (11% increase in loaded vs control limb) compared to ZT2 (8% increase). Similar trends in loaded vs control limb differences between ZT2 and ZT14 mice were observed in cortical thickness (p=0.07) and marrow area (p=0.06). To control for baseline handedness, we also calculated change from baseline in unregistered microCT parameters. We observed that the change from baseline (Δ=day15-day0) in loaded limbs compared to control limbs was significantly greater at ZT14 than ZT2 in ΔCt.Ar/Tt.Ar, ΔMa.Ar, and ΔCtTh (Supplemental Fig. 1). Histomorphometry, however, did not indicate any differences attributable to zeitgeber time (Supplemental Fig. 2; Supplemental Table 1).

Unlike in the cortical midshaft, analysis of the metaphyseal cortical bone and trabecular bone did not reveal any significant differences attributable to zeitgeber time in 3D registered time-lapse morphometry, unregistered microCT parameters, or histomorphometry (Table 2).

Background activity was largely similar between mice loaded at ZT 2 and ZT 14

After excluding the first 24 hours of activity from our analysis, which we considered acclimatization to the metabolic cages, total activity during dark and light phases were compared between both ZT2-loaded and ZT14-loaded mice. Significant differences between mice were only observed on day 9 (light-phase) and day 12 (dark-phase) (Fig. 4). Next, we compared activity onset and offset in mice loaded at ZT2 and ZT14. We observed no significant differences (data not shown).

Although we observed no significant differences in the overall activity rhythms of mice, we analyzed activity in the period immediately following loading. On days when mice were loaded, ZT14-loaded mice exhibited a smaller proportion of their daily activity at ZT14.5-16.5 (the interval immediately following loading) than their ZT2-loaded counterparts (Fig. 4). In contrast, mice loaded at ZT2 did not exhibit a significant difference in activity at ZT2.5-4.5 (immediately after loading) compared to ZT14-loaded mice. On days where mice were not loaded, no significant differences between mice loaded at ZT2 and ZT14 were observed during either interval.

Osteoblast, osteocyte and circadian clock-related genes exhibit diurnal rhythms

We investigated the expression profiles of several circadian rhythm genes over the course of a day by qPCR in sham loaded mouse tibiae. The tibiae were dissected and only the cortical bone was kept to generate osteocyte-enriched samples for RNA extraction. We observed that *Per1* and *Per2* were less expressed at the beginning of the day, and that their expression levels increased to peak early in the night, at ZT14 (Fig. 5a). Inversely, *Arntl1* (*Bmal1*) and *Clock* expression levels were lower at the end of day and increased over night to reach their maximum at ZT22-24 (Fig. 5a). Cosinor analysis confirmed significant rhythmicity in *Per1, Per2, Bmal1,* and *Clock* with a period of 24h (Fig. 5a).

Next, we examined bone turnover genes. We observed that both osteocyte mechanoresponsive genes *Sost* and *Dkk1* had significantly higher expression levels at night, peaking around ZT18 and exhibited significant circadian rhythmic expression profiles, as demonstrated through cosinor analysis (Fig. 5b). *Runx2* and *Bglap* displayed significant 24-hour rhythms as indicated by cosinor analysis, although osteoblast markers *Bglap, Runx2* and *Sp7* did not display significant differences between timepoints (Fig. 5b). Since the *Wnt* signaling pathway is important for regulating bone homeostasis and the anabolic response to mechanical loading, we examined two of its effectors. However, no cyclic pattern was observed for *Lef 1* nor *Axin2* expression in these tibiae cortices.

RNA extracts from the bone marrow of the same bones were then used to study osteoclast gene expression over a 24-hour period. We observed that *Ctsk* and *Acp5* (*Trap5*) did not significantly differ in their expression at different time points and no significant diurnal rhythm was observed (data not shown).

Serum bone turnover markers did not exhibit rhythmicity

We examined serum samples of the sham-loaded mice to establish rhythmicity of sclerostin, P1NP, and TRAP5B. We observed no significant circadian rhythms in any of these proteins, nor any statistical differences between timepoints (Fig. 6).

Sost expression after loading is affected by time of day

Mice that were loaded at ZT14 showed sustained downregulation of *Sost* gene expression in the loaded limb compared to the contralateral control limb (Fig. 7). We detected lower *Sost* mRNA levels 1h, 8h and 24h after loading, although not statistically significant at 8h ($p=0.06$). Strikingly, we saw that *Sost* gene expression behaved differently when tibiae were loaded at ZT2: relative mRNA levels remained unchanged 1h and 24h after loading and were even significantly increased 8h after loading (Fig. 7).

Similarly, we observed that mice that were loaded at ZT14 displayed downregulation of *Dkk1* expression 1h and 24h after loading (Fig. 7). Mice that were loaded at ZT2, on the other hand, displayed no differences in relative *Dkk1* mRNA at 1h, 8h, or 24h after loading.

Discussion

The aim of the present study was to investigate the potential effects of circadian rhythms on load-induced bone formation in mice. We hypothesized that 1) time of day would affect the bone formation and resorption response to mechanical loading at the tissue level and that 2) bone formation and resorption in response to mechanical loading is regulated by circadian rhythms

through peripheral clocks in osteocytes. Using a well-established loading protocol (Main et al., 2020; Willie et al., 2013) we employed 3D registered microCT-based time-lapse morphometry to quantify the anabolic and catabolic response to *in vivo* mechanical loading.

In support of our first hypothesis, we show that the diaphyseal cortical bone formation and resorption response to loading is influenced by the time of day at which loading is administered. We demonstrate that the diaphyseal cortical bone formation response to loading was significantly greater in mice loaded at ZT14 (active phase) than those loaded at ZT2 (resting phase). We observe a greater percent increase in the volume of newly mineralized endocortical bone ($Ec.MV/BV_{day0\text{-}15}$) in response to loading at ZT14 (276%, loaded vs control limb) than loading at ZT2 (72%, $p<0.01$). A similar response was observed in the newly formed endocortical bone surface ($Ec.MS/BS_{day0\text{-}15}$) with a 292% increase in ZT14 mice (loaded vs control) compared to a 95% increase in ZT2 mice ($p=0.07$) (Fig. 2; Table 1) and for newly mineralized thickness ($Ec.MTh_{day0\text{-}15}$, $p=0.06$) (Fig. 2; Table 1).

Mice undergo surface modeling and remodeling, and very rarely experience intracortical remodeling (Piemontese et al., 2017). We observed dramatic differences in endocortical and periosteal responses to loading based on the time of day, with the endocortical being much more pronounced in the young growing mice. We have previously observed that the endocortical bone is more mechanoresponsive than the periosteal (Birkhold et al., 2016), which recent data indicates is related to differences in fluid flow influenced by osteocyte lacunar canalicular network architecture. There was no significant interaction observed between loading and zeitgeber time for conventional microCT bone microstructure parameters, which reflect changes in the whole bone. Also, the unregistered day 0 and 15 images used for this analysis may have examined slightly different bone regions since the young animals experience longitudinal growth

(Birkhold et al., 2014a; Lan et al., 2013). We also did not observe an effect of zeitgeber time on diaphyseal cortical bone formation with conventional histomorphometry, nor did we see a significant effect of loading in most histomorphometry parameters. Although histomorphometry allows for the endocortical and periosteal surfaces to be analyzed separately, it only examines a single two-dimensional slice within the bone volume, while microCT-based time-lapse morphometry allows for an entire volume of interest, in our case 10% of the bone length. We previously showed that mineral apposition rates can vary dramatically throughout this volume of interest (Birkhold et al., 2014a), which may explain our results.

Interestingly, our time of day effects were site-specific and not observed in the metaphyseal cortical nor trabecular bone. The site-specific differences might be due to differences in local tissue strains, fluid flow, or sclerostin abundance (Moustafa et al., 2012). We observed a greater bone formation response to loading in the diaphyseal cortical bone (185% increase in $Ec.MV/BV_{day0\text{-}15}$ in loaded vs control limbs) compared to the metaphyseal cortical bone (32% increase in $Ec.MV/BV_{day0\text{-}15}$ in loaded vs control limbs). We and others have showed using *in vivo* strain gauging and finite element modeling that the 50% cortical bone mid-diaphyseal region of the tibia experiences much higher strain magnitudes during *in vivo* loading than the metaphyseal region (Albiol et al., 2018; Birkhold, Razi, Duda, Checa, & Willie, 2017; Patel, Brodt, & Silva, 2014; Razi et al., 2015).

In support of our second hypothesis, we observed that *Sost* and *Dkk1* gene expression was differentially expressed after loading, depending on the time of day at which mechanical loading was applied. Mice that were loaded at ZT2 (resting phase) displayed increases in *Sost* expression

in loaded limbs compared to control limbs 8 hours after loading, while mice loaded at ZT14 (active phase) displayed decreases in *Sost* expression in loaded limbs 1, 8 ($p=0.06$), and 24 hours after loading and decreases in *Dkk1* expression in loaded limbs 1 and 24 hours after loading (Fig. 7). Robling et al. originally reported that *Sost* gene expression and sclerostin protein expression were downregulated with mechanical loading in ulnae of mice (Robling et al., 2008). While we also observed decreases in *Sost* expression in our previous experiments, some of our previous data (Pflanz et al., 2017) and those reported by others (Chermside-Scabbo et al., 2020) have shown inconsistent downregulation of *Sost* expression after loading. Our results indicate that time of day plays a crucial role in *Sost* and *Dkk1* regulation. Previous studies have not reported the time of day at which mice were loaded or euthanized for collection of RNA, which may explain the variability in the gene expression data reported. Thus, our results indicate that care should be taken to always load mice at the same time of day to prevent biasing results, and that loading mice during the evening (active phase) results in an increased bone formation response compared to the morning (resting phase). Although the selection of these two ZT times was somewhat arbitrary and thus ongoing studies are aimed at determining if loading at other ZTs results in more enhanced bone mechanoadaptation.

For the first time, we show a diurnal expression of *Wnt* signaling inhibiting genes *Sost* and *Dkk1*, suggesting they are clock controlled genes (Fig. 5). This is significant because the downregulation of *Sost* has been implicated as being at least partially responsible for the anabolic response to loading(Tu et al., 2012). In addition, to loading, parathyroid hormone (PTH) also reduces *Sost* gene levels in bone (Bellido et al., 2005; Kramer, Loots, Studer, Keller, & Kneissel, 2010). It has been proposed that PTH signaling in osteocytes influences skeletal remodeling by coordinated transcriptional regulation of paracrine mediator, *Sost* (Kramer, Keller, Leupin, &

Kneissel, 2010; Wein, 2018). It has been previously demonstrated in human serum samples that parathyroid hormone (PTH) expresses a diurnal rhythm displaying a peak in expression in the late-night/early-morning and a minimum in the mid-morning (Jubiz, Canterbury, Reiss, & Tyler, 1972). PTH acts synergistically with loading to increase load-induced bone formation (Fahlgren et al., 2013; Grosso et al., 2015; Li, Duncan, Burr, Gattone, & Turner, 2003). A clinical study showed 12 month daily PTH administration increased BMD when administered in the morning compared to the evening (Michalska et al., 2012). PTH has also been shown to target *Sost* in bone, and *Sost* knockout mice display a blunted response to PTH induced bone formation (Keller & Kneissel, 2005; Kramer, Loots, et al., 2010). The oscillation of *Sost* mRNA we observed might be related to the oscillatory profile of PTH, or PTH acts as a timing cue to entrain the peripheral clock of bone to the central circadian clock. Since PTH (teriparatide, recombinant DNA origin human PTH (1-34)) and sclerostin neutralizing antibody (Scl-Ab) are the only FDA-available anabolic pharmaceutical therapies to treat low bone mass conditions, our findings highlight the need to understand the influence of circadian rhythms on signaling pathways that regulate bone formation.

Bone specific genes *Bglap,* and *Runx2* also displayed a rhythmic expression, however serum levels for sclerostin, P1NP, and TRAP5B were not rhythmic (Figs. 5 and 6). Previous experiments have reported the presence of rhythmic expression of osteoclast specific genes in mouse cell culture, and the presence of rhythmic bone turnover markers in human sera and plasma (Fujihara et al., 2014; Greenspan et al., 1997; C. Swanson et al., 2017; van der Spoel et al., 2019). It has also been shown in mice at the mRNA level that FGF-23, Rankl, Opg, and Ctsk have a diurnal rhythm (Kawai, Kinoshita, Shimba, Ozono, & Michigami, 2014; Schilperoort et al., 2020). Studies in mice have shown that serum osteocalcin and CTX exhibit a diurnal rhythm,

but not skeletal alkaline phosphotase (sALP) (Srivastava, Bhattacharyya, Li, Mohan, & Baylink, 2001). Studies analyzing human serum have reported contradictory results regarding the presence or absence of a diurnal rhythm in P1NP, which may be the case for mice as well (Swanson et al., 2018). There is also debate as to whether or not sclerostin is rhythmic in serum (Santosh H Shankarnarayan, 2013; C. Swanson et al., 2017; van der Spoel et al., 2019). Despite this discrepancy, it remains unclear whether serum and plasma levels of these proteins adequately represent important mRNA dynamics in the bone itself (Delgado-Calle et al., 2017; Roforth et al., 2014). Our results indicate that serum sclerostin is not an accurate marker of sclerostin dynamics in bone and highlight the importance of taking time of day into account when analyzing gene expression data, further implicating circadian rhythm involvement in bone. Additionally, these data may indicate that sclerostin acts in bone in a paracrine manner, therefore serum levels may not be relevant.

In support of our second hypothesis, we showed that core circadian clock genes exhibited cyclic expression profiles in osteocyte-rich cortical bone. Mineral deposition in calvaria, collagen turnover, and fracture healing have been shown to express circadian rhythms (Chang et al., 2020; Kunimoto et al., 2016; McElderry et al., 2013). These tissue level effects have been corroborated by the effects of various clock gene global knockouts on bone: *Bmal1* knockout results in low bone mass phenotypes, *Per1, Per2*, and *Cry2* knockouts result in high bone mass phenotypes (Fu et al., 2005; Maronde et al., 2010; Samsa et al., 2016). In addition, the effect of clock genes specifically in osteoblasts and osteoclasts have been identified through conditional knockouts of *Bmal1* in osteoblasts as well as *Bmal1* rhythms in osteoclast cell culture (Fujihara et al., 2014; Samsa et al., 2016). Despite robust evidence for clock gene effects on osteoblasts and

osteoclasts, little is known regarding osteocytes. The only other study that reported clock gene expression in osteocytes, by Takarada et al. (Takarada et al., 2017) showed peaks in *Bmal1* expression in murine calvaria at ZT20 and peaks in *Per1* at ZT12. Although our gene expression results are from tibiae, we saw similar peaks in *Bmal1* at ZT2 and peaks in *Per1* at ZT14. Slight differences between peak times may be the result of different dissection times between the studies, different mouse age at time of dissection, or mouse strains. Our results demonstrate robust clock gene rhythms in osteocyte-rich bone samples.

A previous experiment suggested that background activity can mask load-induced bone formation. Meakins et al. (Meakin et al., 2013) reported that group housing and the subsequent frequent fighting observed in male mice led to diminished loading effects compared to single-housed mice, attributing the difference to added strain engendered in the bones during fighting. Mice are nocturnal; thus, their active phase occurs during the night (ZT12-24) and loading at ZT14 may add to the higher background loads occurring naturally during the night. To ensure both that the circadian rhythms of our mice remained undisturbed, and to quantify the effects of background loading, we for the first time measured the background activity of mice during an *in vivo* tibial loading experiment. We found that there were no significant changes in the onset and offset of background activity, suggesting that the global circadian rhythms of our mice remained unchanged by the in vivo loading at different times of day (Fig. 4E, F). We observed no significant differences in the total activity of ZT2 loaded and ZT14 loaded mice, further confirming that background loading was equivalent in our mice (Fig. 4C, D). In addition, the mice that displayed greater cortical bone formation (ZT14 mice), also displayed a decrease in activity immediately post-loading compared to their ZT2 counterparts, indicating that background loading was not responsible for the increased cortical bone formation observed in

ZT14 compared to ZT2 loaded mice (Fig. 4A, B). Based on these results and a previous study showing that loading and exercise do not have additive effects in cortical bone (Berman, Hinton, & Wallace, 2019), we believe our differences in cortical bone response to mechanical loading at different zeitgeber times can be solely attributed to the oscillatory gene expression we observed.

Our study has limitations. Our tissue level study only performed loading at two time points, ZT2 and ZT14. These times were selected based on the lighting schedule, where the light phase started at ZT0 and the dark phase started at ZT12. Having the experimental time points two hours after the initiation of light and dark phase, allowed us to avoid the transition periods, and examine the animals during a fully light or dark phase. While these time points were selected with the intention to see significant differences, it is possible that the greatest changes in osteocyte gene expression occur at different moments in the day, thus the observed changes are only a portion of the picture. Future work is needed to examine tissue-level changes due to mechanical loading at more time points, to better understand the oscillatory bone formation response to loading at multiple times of day. We did not measure serum samples of PTH or other hormones in our 2-week loaded mice, as they were dissected at the same zeitgeber time. Studies are ongoing to determine if signaling pathways known to have circadian rhythms, such as PTH expression may play a role in peripheral clock directed, load-induced bone formation. We extracted RNA from osteocyte-rich cortical bone, but it may contain some osteoblasts and osteoclasts. However, alternative approaches to selectively study osteocytic versus osteoblastic gene expression use extended collagenase digestions procedures (Halleux, Kramer, Allard, & Kneissel, 2012; Stern et al., 2012), which likely impact the circadian phase.

Our key findings are: 1) the diaphyseal cortical bone formation response to mechanical loading is increased in mice loaded at ZT14 compared to mice loaded at ZT2. 2) Both central clock genes

such *as Bmal1* and *Per2* as well as osteocyte specific genes *Sost* and *Dkk1* express robust gene expression rhythms in cortical bone. 3) *Sost* is downregulated 1, 8 (p=0.06), and 24-hours post-loading in ZT14 mice, but upregulated 8-hours post-loading in ZT2 mice. Similarly, *Dkk1* is also downregulated 1h and 24h post-loading in ZT14 mice, but unchanged in ZT2 mice. We demonstrate differences in bone mechanoresponse at both the molecular and tissue-level. These data suggest that mice loaded at night (ZT14, active phase) had a greater cortical bone formation response to *in vivo* mechanical loading than mice loaded during the day (ZT 2, resting phase). Since mice are nocturnal (active at night), translating our results to humans will require focusing on active compared to resting phases in both species. *F*urther experiments are needed to establish the implications for humans. It is also unclear if diurnal rhythms of bone formation and resorption and gene expression (eg. *Sost*) follows the same rhythms in mice and humans. Further studies are warranted to determine how the circadian clock regulates osteocyte-related genes and bone mass. This knowledge will allow us to optimize current treatments as well as identify novel molecular targets that can be used as countermeasures for serious problems caused by severe lack in physical activity in frail elderly and paralyzed patients, who suffer from loss of muscle and bone, and are at high risk of metabolic disorders and low-trauma fractures.

Materials and Methods

Animals for two-week tibial loading

Twenty-one, 10-week old female C57BL/6J mice (Jackson Laboratories, Bar Harbour, ME, USA) were received and acclimatized in the animal facility at the Shriner's Hospital for Children. After acclimatization, mice were housed singly in metabolic cages (OxyMax CLAMS,

OH, USA) with *ad libitum* access to food and water, and 12:12hr light-dark cycle with the light period beginning at 6:00 and ending at 18:00. These mice remained in the metabolic cages for the entirety of the experiment (20 days) and were removed temporarily from the cages only for *in vivo* loading, *in vivo* imaging, and cleaning of the cages. This recording time allowed for acclimatizing to the cages (24 hours) followed by 4 days of background activity measurement prior to the start of the loading protocol (Fig. 1a). Outcome parameters of the metabolic cages included activity counts (xamb, xtot, ztot) as well as metabolic parameters. Two mice were sacrificed immediately after their first loading bout as incorrect positioning led to tibial fractures. Otherwise, all mice tolerated the experiment well. All animal use was approved by the Shriner's Facility Animal Care Committee (AUP 2016-7281), which abide by guidelines and policies from the Canadian Council on Animal Care.

Two-week in vivo tibial loading

The left tibiae of each mouse underwent in vivo cyclic compressive loading either in the light phase at ZT2, 8:00 (n=9 mice) or in the dark phase at ZT14, 20:00 (n=10 mice). Loading was performed as previously described (Birkhold et al., 2014a; Willie et al., 2013). Briefly, mice were anesthetized during loading using isoflurane (2% in 2.0 L/min O_2). The left knee of each mouse was placed in a concave cup and its foot rested on a platen. A preload of -1N was applied to prevent the tibia from moving out of the fixtures. Loading parameters included 216 cycles applied daily at 4Hz, 5 days/week for two weeks, delivering -11N peak loads. Previous *in vivo* strain gauge studies in our lab have shown that this load level engenders 1200 με at the antero-medial surface of the tibial midshaft in ten-week-old female C57BL/6J mice (Birkhold et al., 2014a; Willie et al., 2013). The right tibia of each mouse served as a nonloaded control.

Importantly, mice loaded during the dark phase (ZT14) were handled in dim red light to avoid disrupting the circadian rhythm.

In vivo microCT imaging

In vivo microCT at an isotropic voxel size of 8.0 µm (SkyScan 1276, Bruker; 70 kVp, 57 µA, 0.3° rotation step, 0.5mm Al filter) was performed every 5 days, beginning one day prior to the first loading session (days 0, 5, 10, 15) (Fig. 1). Mice were anesthetized with isofluorane during the scan (2% in 0.6 L/min O_2) and kept in a fixed position using a custom-made mouse bed. Each scan captured the entire length of the tibia and took approximately 20 minutes per mouse. Accumulated radiation dose per scan was estimated to be 150mGy.

3D registered Micro-CT based time-lapse morphometry

Three-dimensional image registration and time-lapse morphometry was performed as previously described by Birkhold et al. (Birkhold et al., 2014a). Micro computed tomography (µCT) images of both tibias of each mouse were taken every 5 days (day 0, 5, 10, 15) and evaluated to determine bone morphological changes due to growth and loading-related adaptation (Birkhold et al., 2014b). Briefly, microCT scans was reconstructed and segmented into the desired vertical volumes of interest (VOI). The metaphyseal VOI was defined as beginning 104µm below the growth plate and extending distally 10% of the bone length. The 50% VOI was defined as 2.5% proximal and distal to the mid-shaft slice (50% of the bone length). In the metaphyseal region, the trabecular bone compartment inside the medullary area was excluded from cortical bone analyses. A global threshold of 0.84g/cm^3 at the midshaft and 0.56g/cm^3 at the metaphyseal region were used to segment cortical bone from soft tissue. A global threshold of 0.46g/cm^3 was used to segment trabecular bone from soft tissue. The fibula was removed from each image prior

to registration, and consecutive microCT images were aligned geometrically using Amira (FEI, SAS, France). After registering images, the coordinate system of the latter-day scans were transformed onto the reference day coordinate system, and images were cropped into previously described VOIs. Images were then post-processed using scripts written in Matlab (Matlab 2016b; The Mathworks, Inc. Natick, MA, USA). Images were compared voxel by voxel, labeling bone only present on later days as formed, bone only present on reference day images as resorbed, and bone present in both images as quiescent. Dynamic histomorphometry outcome parameters included: mineralized bone volume (MV/BV), mineralized bone surface (MS/BS), eroded bone volume (EV/BV), eroded bone surface (ES/BS), mineralized thickness (MTh), and eroded depth (ED). One mouse was excluded from analysis due to an overabundance of movement artifact.

Unregistered microCT analysis

Cortical bone outcome parameters analyzed included principal moments of inertia (Imax, Imin), cortical bone area = cortical volume/ (number of slices * slice thickness) (Ct.Ar), total cross-sectional area inside the periosteal envelope (Tt.Ar), cortical area fraction (Ct.Ar/Tt.Ar), cortical thickness (Ct.Th), and cortical volumetric tissue mineral density (Ct.vTMD) as recommended (Bouxsein et al., 2010). Trabecular bone outcome parameters included: bone volume fraction (BV/TV), trabecular thickness (Tb.Th), average number of trabeculae per unit length (Tb.N), trabecular separation (Tb.Sp), and trabecular volumetric tissue mineral density (Tb.vTMD) as recommended (Bouxsein et al., 2010).

Dynamic histomorphometry

Mice were administered calcein (30mg/kg) 11 and 2 days before euthanasia via intraperitoneal injection. After dissection, bones were fixed in 70% ethanol and dehydrated in ascending grades

of ethanol. They were then embedded in polymethyl methacrylate. The embedded bones were sectioned at the mid-shaft in the transverse plane and in the sagittal plane of the proximal tibia, to analyze both cortical and trabecular bone. Sections were imaged at 20x magnification using a confocal laser scanning microscope (Zeiss LSM780). Confocal microscope images were analyzed using Bioquant Osteo (BIOQUANT Image Analysis Corporation, Nashville, TN). Cortical and trabecular bone was analyzed for single and double-labeled surfaces (sLS/BS, dLS/BS), mineral apposition rate (MAR), mineralizing surface per bone surface (MS/BS) and bone-formation rate per bone surface (BFR/BS) as recommended(A. M. Parfitt et al., 1987). MS/BS was calculated using the formula 0.5*sLS/BS + dLS/BS. In sections where double-labeled surfaces were not present, ie dLS/BS = 0, this sample did not contribute to MAR or BFR/BS. One sample was excluded as the bone was broken during the embedding process.

Activity Data

Activity data counts were measured in OxyMax CLAMS cages, described above. Activity onset and offset were calculated using average actograms generated with actogramJ (Schmid, Helfrich-Forster, & Yoshii, 2011). Acute activity post-loading was defined as a proportion of daily activity during the 2-hours after loading (ZT2.5-4.5 and ZT14.5-16.5). This proportion was compared on 4 loaded days and 4 non-loaded days. Total light-phase, dark-phase, and whole-day activity were also compared between ZT2 and ZT14 mice.

Animals for single tibial loading session

Seventy-Two, 10-week old female C57BL/6J mice (Jackson Laboratories, Bar Harbour, ME, USA) were received and acclimatized in the animal facility at the Shriner's Hospital for Children. Mice were group housed 3 per cage, with ad libitum access to food and water, and

12:12hr L/D light cycle with the light period beginning at 6:00 and ending at 18:00. All animal use was approved by the Shriner's Facility Animal Care Committee (AUP 2016-7821).

Single in vivo tibial loading session

Seventy-two mice were randomly assigned to be loaded (36 mice) or sham loaded (36 mice). The left tibia of each mouse underwent in vivo cyclic compressive loading either in the light phase at ZT2, 8:00 (n=18 mice) or in the dark phase at ZT14, 20:00 (n=18 mice). Loading was performed as described above. Peak loads of -11N were delivered, and the right tibia served as nonloaded control. The sham loaded mice were anesthetized for the same duration as loaded mice (~5 mins) at ZT2,6,10,14,18,22 (n=6/timepoint) but were not loaded. All sham loaded mice were dissected 8-hours after being anesthetized.

Gene expression analysis

After being subjected to a single bout of in-vivo mechanical loading or sham-loading (anesthesia only) mice were sacrificed 1, 8, or 24 hours post-loading to measure early, middle, and late responding genes (sham-loaded mice were all sacrificed at 8h after). The left and right tibial cortices of each animal (n=5-6 mice/ group) were dissected by first removing both epiphyses and proximal trabecular bone. Bone marrow was then flushed in separate tubes using RNA-later (Qiagen). Samples were flash frozen in liquid nitrogen and stored at -80°C. RNA was extracted with Aurum total RNA fatty and fibrous tissue kit (BioRad). Samples were reverse-transcribed with high-capacity cDNA reverse transcription kit (Thermo-Fisher). Gene expression was determined using a QuantStudio™ 7 Flex system, TaqMan® Fast Advanced Master Mix and the following TaqMan® probes (Thermo-Fisher) (Table 1). GAPDH (Mm99999915_g1) and Hprt (Mm03024075_m1) (averaged) were used for normalization.

ELISA

Thirty-six mice were sham-loaded (as described above) and dissected 8 hours after sham-loading. Blood was collected by cardiac puncture, allowed to clot, and spun at 10,000 rpm for 5 minutes. Serum was collected and stored at -80°C. Serum concentrations of Sclerostin, P1NP, and TRAP5b were measured using Enzyme Linked Immunosorbent Assay according to the manufacturers protocol. The Sclerostin protocol, Mouse\Rat SOST\Sclerostin Quantikine ELISA (R&D Systems, Minneapolis, MN, catalog no. MSST00), was modified to use 20ul (instead of 50ul) and values generated remained in the range of sensitivity for this kit. The TRAP5b protocol (IDS immunodiagnosticsystems, Boldon, UK, catalog no. SB-TR103) was modified to require 20ul of sample (instead of 25ul), and values obtained remined in the range of sensitivity of this kit. The P1NP protocol (IDS immunodiagnosticsystems, Boldon, UK, catalog no. AC-33F1) remined unmodified. When possible, all samples were assayed in duplicate.

Statistical analysis

Normality was assessed using a Shapiro-Wilk test and variance was assessed using a folded F test. The within-subject effect of loading and injection (loaded, control limb) and between-subject effects time of loading (ZT2, ZT14) as well as interactions between these terms was assessed using a repeated measures ANOVA (SAS 9.4, Cary, USA) for absolute values. Relative values (within-limb difference = day 15 – day0) were analyzed using a repeated measures ANOVA in animals with significant baseline differences (handedness). Tukey-kramer post-hoc test was used to test for time of day differences in loaded limbs. For qPCR and ELISA analysis, one-way ANOVA was used to measure effect of Zeitgeber Time, and standard cosinor analysis was used to confirm rhythmicity (Bingham, Arbogast, Guillaume, Lee, & Halberg, 1982;

Refinetti, Lissen, & Halberg, 2007). Paired t-tests were used to compare *Sost* and *Dkk1* expression after loading. A p value < 0.05 was considered significant. Unless otherwise indicated all results reported were significant, $p < 0.05$, and presented as mean ± standard deviation. All p-values <0.1 are indicated on figures.

Acknowledgments

The authors thank Nicolas Cermakian, Suzanne Morin, and Tobias Thiele for thoughtful discussions. We also thank Tara Delorme, Annie-Laurine Sezikeye, Kira Sikorska, and Jenna Tetrault and for experimental assistance. We thank Mark Lepik for assistance with illustrations. This study was supported by a grant from the Shriners Hospitals for Children and the FRQS Programme de bourses de chercheur.

Disclosures

The authors have nothing to disclose.

References

1. B. M. Willie, E. A. Zimmermann, I. Vitienes, R. P. Main, S. V. Komarova, Bone adaptation: Safety factors and load predictability in shaping skeletal form. *Bone* **131**, 115114 (2020).

2. P. Pivonka, *Multiscale Mechanobiology of Bone Remodeling and Adaptation* (Springer, 2018).

3. H. H. Jones, J. D. Priest, W. C. Hayes, C. C. Tichenor, D. A. Nagel, Humeral hypertrophy in response to exercise. *J Bone Joint Surg Am* **59**, 204-208 (1977).

4. A. M. Schroeder *et al.*, Voluntary scheduled exercise alters diurnal rhythms of behaviour, physiology and gene expression in wild-type and vasoactive intestinal peptide-deficient mice. *J Physiol* **590**, 6213-6226 (2012).

5. G. Wolff, K. A. Esser, Scheduled exercise phase shifts the circadian clock in skeletal muscle. *Med Sci Sports Exerc* **44**, 1663-1670 (2012).

6. L. Bonewald, Use it or lose it to age: A review of bone and muscle communication. *Bone* **120**, 212-218 (2019).

7. C. Oudet, A. Petrovic, J. Stutzmann, Time-dependent effects of a 'functional'-type orthopedic appliance on the rat mandible growth. *Chronobiol Int* **1**, 51-57 (1984).

8. K. Miyoshi, K. Igarashi, S. Saeki, H. Shinoda, H. Mitani, Tooth movement and changes in periodontal tissue in response to orthodontic force in rats vary depending on the time of day the force is applied. *Eur J Orthod* **23**, 329-338 (2001).

9. M. Hastings, The brain, circadian rhythms, and clock genes. *BMJ* **317**, 1704-1707 (1998).

10. M. H. Hastings, E. D. Herzog, Clock genes, oscillators, and cellular networks in the suprachiasmatic nuclei. *J Biol Rhythms* **19**, 400-413 (2004).

11. S. M. Reppert, D. R. Weaver, Coordination of circadian timing in mammals. *Nature* **418**, 935-941 (2002).

12. G. Asher, U. Schibler, Crosstalk between components of circadian and metabolic cycles in mammals. *Cell Metab* **13**, 125-137 (2011).

13. C. Dibner, U. Schibler, U. Albrecht, The mammalian circadian timing system: organization and coordination of central and peripheral clocks. *Annu Rev Physiol* **72**, 517-549 (2010).

14. T. Hirai, K. Tanaka, A. Togari, beta-adrenergic receptor signaling regulates Ptgs2 by driving circadian gene expression in osteoblasts. *J Cell Sci* **127**, 3711-3719 (2014).

15. S. Komoto, H. Kondo, O. Fukuta, A. Togari, Comparison of beta-adrenergic and glucocorticoid signaling on clock gene and osteoblast-related gene expressions in human osteoblast. *Chronobiol Int* **29**, 66-74 (2012).

16. Y. Fujihara, H. Kondo, T. Noguchi, A. Togari, Glucocorticoids mediate circadian timing in peripheral osteoclasts resulting in the circadian expression rhythm of osteoclast-related genes. *Bone* **61**, 1-9 (2014).

17. T. M. Skerry, L. Bitensky, J. Chayen, L. E. Lanyon, Early strain-related changes in enzyme activity in osteocytes following bone loading in vivo. *J Bone Miner Res* **4**, 783-788 (1989).

18. T. Inaoka *et al.*, Sequential analysis of gene expression after an osteogenic stimulus: c-fos expression is induced in osteocytes. *Biochem Biophys Res Commun* **217**, 264-270 (1995).

19. A. M. Parfitt, "Skeletal Heterogeneity and the Purposes of Bone Remodeling: Implications for the Understanding of Osteoporosis" in Osteoporosis (Forth Edition), D. F. Robert Marcus, David W. Dempster, Majorie Luckey, Jane A. Cauley Ed. (Academic Press, 2013), chap. 36, pp. 855-872.

20. S. H. Yoo *et al.*, PERIOD2::LUCIFERASE real-time reporting of circadian dynamics reveals persistent circadian oscillations in mouse peripheral tissues. *Proc Natl Acad Sci U S A* **101**, 5339-5346 (2004).

21. J. S. Takahashi, H. K. Hong, C. H. Ko, E. L. McDearmon, The genetics of mammalian circadian order and disorder: implications for physiology and disease. *Nat Rev Genet* **9**, 764-775 (2008).

22. L. Fu, M. S. Patel, A. Bradley, E. F. Wagner, G. Karsenty, The molecular clock mediates leptin-regulated bone formation. *Cell* **122**, 803-815 (2005).

23. T. Takarada *et al.*, Bone Resorption Is Regulated by Circadian Clock in Osteoblasts. *J Bone Miner Res* **32**, 872-881 (2017).

24. C. Xu *et al.*, Circadian Clock Regulates Bone Resorption in Mice. *J Bone Miner Res* **31**, 1344-1355 (2016).

25. J. D. McElderry *et al.*, Tracking circadian rhythms of bone mineral deposition in murine calvarial organ cultures. *J Bone Miner Res* **28**, 1846-1854 (2013).

26. C. Swanson *et al.*, 24-hour profile of serum sclerostin and its association with bone biomarkers in men. *Osteoporos Int* **28**, 3205-3213 (2017).

27. P. Qvist, S. Christgau, B. J. Pedersen, A. Schlemmer, C. Christiansen, Circadian variation in the serum concentration of C-terminal telopeptide of type I collagen (serum CTx): effects of gender, age, menopausal status, posture, daylight, serum cortisol, and fasting. *Bone* **31**, 57-61 (2002).

28. J. Redmond *et al.*, Diurnal Rhythms of Bone Turnover Markers in Three Ethnic Groups. *J Clin Endocrinol Metab* **101**, 3222-3230 (2016).

29. M. Luchavova *et al.*, The effect of timing of teriparatide treatment on the circadian rhythm of bone turnover in postmenopausal osteoporosis. *Eur J Endocrinol* **164**, 643-648 (2011).

30. E. van der Spoel *et al.*, The 24-hour serum profiles of bone markers in healthy older men and women. *Bone* **120**, 61-69 (2019).

31. S. L. Greenspan, R. Dresner-Pollak, R. A. Parker, D. London, L. Ferguson, Diurnal variation of bone mineral turnover in elderly men and women. *Calcif Tissue Int* **60**, 419-423 (1997).

32. A. R. Santosh HS, Hamilton A, Barraclough DL, Fraser WD, Vora JP (2013) Circadian rhythm of circulating sclerostin in healthy young men. . in *15th European congress of endocrinology.* (Copenhagen, Denmark), p 72.

33. C. M. Swanson *et al.*, Bone Turnover Markers After Sleep Restriction and Circadian Disruption: A Mechanism for Sleep-Related Bone Loss in Humans. *J Clin Endocrinol Metab* **102**, 3722-3730 (2017).

34. R. P. Main *et al.*, Murine Axial Compression Tibial Loading Model to Study Bone Mechanobiology: Implementing the Model and Reporting Results. *J Orthop Res* **38**, 233-252 (2020).

35. B. M. Willie *et al.*, Diminished response to in vivo mechanical loading in trabecular and not cortical bone in adulthood of female C57Bl/6 mice coincides with a reduction in deformation to load. *Bone* **55**, 335-346 (2013).

36. M. Piemontese *et al.*, Old age causes de novo intracortical bone remodeling and porosity in mice. *JCI Insight* **2** (2017).

37. A. I. Birkhold *et al.*, The Periosteal Bone Surface is Less Mechano-Responsive than the Endocortical. *Sci Rep* **6**, 23480 (2016).

38. A. I. Birkhold *et al.*, The influence of age on adaptive bone formation and bone resorption. *Biomaterials* **35**, 9290-9301 (2014).

39. S. Lan *et al.*, 3D image registration is critical to ensure accurate detection of longitudinal changes in trabecular bone density, microstructure, and stiffness measurements in rat tibiae by in vivo microcomputed tomography (muCT). *Bone* **56**, 83-90 (2013).

40. A. Moustafa *et al.*, Mechanical loading-related changes in osteocyte sclerostin expression in mice are more closely associated with the subsequent osteogenic response than the peak strains engendered. *Osteoporos Int* **23**, 1225–1234 (2012).

41. H. Razi *et al.*, Skeletal maturity leads to a reduction in the strain magnitudes induced within the bone: a murine tibia study. *Acta Biomater* **13**, 301-310 (2015).

42. T. K. Patel, M. D. Brodt, M. J. Silva, Experimental and finite element analysis of strains induced by axial tibial compression in young-adult and old female C57Bl/6 mice. *J Biomech* **47**, 451-457 (2014).

43. L. Albiol *et al.*, Sost deficiency leads to reduced mechanical strains at the tibia midshaft in strain-matched in vivo loading experiments in mice. *J R Soc Interface* **15** (2018).

44. A. I. Birkhold, H. Razi, G. N. Duda, S. Checa, B. M. Willie, Tomography-Based Quantification of Regional Differences in Cortical Bone Surface Remodeling and Mechano-Response. *Calcif Tissue Int* **100**, 255-270 (2017).

45. A. G. Robling *et al.*, Mechanical stimulation of bone in vivo reduces osteocyte expression of Sost/sclerostin. *J Biol Chem* **283**, 5866-5875 (2008).

46. D. Pflanz *et al.*, Sost deficiency led to a greater cortical bone formation response to mechanical loading and altered gene expression. *Sci Rep* **7**, 9435 (2017).

47. N. Holguin, M. D. Brodt, M. J. Silva, Activation of Wnt Signaling by Mechanical Loading Is Impaired in the Bone of Old Mice. *J Bone Miner Res* **31**, 2215-2226 (2016).

48. X. Tu *et al.*, Sost downregulation and local Wnt signaling are required for the osteogenic response to mechanical loading. *Bone* **50**, 209-217 (2012).

49. T. Bellido *et al.*, Chronic elevation of parathyroid hormone in mice reduces expression of sclerostin by osteocytes: a novel mechanism for hormonal control of osteoblastogenesis. *Endocrinology* **146**, 4577-4583 (2005).

50. I. Kramer, G. G. Loots, A. Studer, H. Keller, M. Kneissel, Parathyroid hormone (PTH)-induced bone gain is blunted in SOST overexpressing and deficient mice. *J Bone Miner Res* **25**, 178-189 (2010).

51. I. Kramer, H. Keller, O. Leupin, M. Kneissel, Does osteocytic SOST suppression mediate PTH bone anabolism? *Trends Endocrinol Metab* **21**, 237-244 (2010).

52. M. N. Wein, Parathyroid Hormone Signaling in Osteocytes. *JBMR Plus* **2**, 22-30 (2018).

53. W. Jubiz, J. M. Canterbury, E. Reiss, F. H. Tyler, Circadian rhythm in serum parathyroid hormone concentration in human subjects: correlation with serum calcium, phosphate, albumin, and growth hormone levels. *J Clin Invest* **51**, 2040-2046 (1972).

54. J. Li, R. L. Duncan, D. B. Burr, V. H. Gattone, C. H. Turner, Parathyroid hormone enhances mechanically induced bone formation, possibly involving L-type voltage-sensitive calcium channels. *Endocrinology* **144**, 1226-1233 (2003).

55. A. Fahlgren *et al.*, The effects of PTH, loading and surgical insult on cancellous bone at the bone-implant interface in the rabbit. *Bone* **52**, 718-724 (2013).

56. M. J. Grosso *et al.*, Intermittent PTH administration and mechanical loading are anabolic for periprosthetic cancellous bone. *J Orthop Res* **33**, 163-173 (2015).

57. D. Michalska *et al.*, Effects of morning vs. evening teriparatide injection on bone mineral density and bone turnover markers in postmenopausal osteoporosis. *Osteoporos Int* **23**, 2885-2891 (2012).

58. H. Keller, M. Kneissel, SOST is a target gene for PTH in bone. *Bone* **37**, 148-158 (2005).

59. M. Kawai, S. Kinoshita, S. Shimba, K. Ozono, T. Michigami, Sympathetic activation induces skeletal Fgf23 expression in a circadian rhythm-dependent manner. *J Biol Chem* **289**, 1457-1466 (2014).

60. M. Schilperoort *et al.*, Circadian disruption by shifting the light-dark cycle negatively affects bone health in mice. *FASEB J* **34**, 1052-1064 (2020).

61. A. K. Srivastava, S. Bhattacharyya, X. Li, S. Mohan, D. J. Baylink, Circadian and longitudinal variation of serum C-telopeptide, osteocalcin, and skeletal alkaline phosphatase in C3H/HeJ mice. *Bone* **29**, 361-367 (2001).

62. C. M. Swanson *et al.*, The importance of the circadian system & sleep for bone health. *Metabolism* **84**, 28-43 (2018).

63. R. A. Santosh H Shankarnarayan, Amanda Hamilton, Dong L Barraclough, William D Fraser & Jiten P Vora (2013) Circadian rhythm of circulating sclerostin in healthy young men. in *15th European Congress of Endocrinology* (European Society of Endocrinology, Copenhagen, Denmark).

64. M. M. Roforth *et al.*, Effects of age on bone mRNA levels of sclerostin and other genes relevant to bone metabolism in humans. *Bone* **59**, 1-6 (2014).

65. J. Delgado-Calle, A. Y. Sato, T. Bellido, Role and mechanism of action of sclerostin in bone. *Bone* **96**, 29-37 (2017).

66. J. Chang *et al.*, Circadian control of the secretory pathway maintains collagen homeostasis. *Nat Cell Biol* **22**, 74-86 (2020).

67. T. Kunimoto *et al.*, A PTH-responsive circadian clock operates in ex vivo mouse femur fracture healing site. *Sci Rep* **6**, 22409 (2016).

68. W. E. Samsa, A. Vasanji, R. J. Midura, R. V. Kondratov, Deficiency of circadian clock protein BMAL1 in mice results in a low bone mass phenotype. *Bone* **84**, 194-203 (2016).

69. E. Maronde *et al.*, The clock genes Period 2 and Cryptochrome 2 differentially balance bone formation. *PLoS One* **5**, e11527 (2010).

70. L. B. Meakin *et al.*, Male mice housed in groups engage in frequent fighting and show a lower response to additional bone loading than females or individually housed males that do not fight. *Bone* **54**, 113-117 (2013).

71. A. G. Berman, M. J. Hinton, J. M. Wallace, Treadmill running and targeted tibial loading differentially improve bone mass in mice. *Bone Rep* **10**, 100195 (2019).

72. C. Halleux, I. Kramer, C. Allard, M. Kneissel, Isolation of mouse osteocytes using cell fractionation for gene expression analysis. *Methods Mol Biol* **816**, 55-66 (2012).

73. A. R. Stern *et al.*, Isolation and culture of primary osteocytes from the long bones of skeletally mature and aged mice. *Biotechniques* **52**, 361-373 (2012).

74. A. I. Birkhold *et al.*, Mineralizing surface is the main target of mechanical stimulation independent of age: 3D dynamic in vivo morphometry. *Bone* **66**, 15-25 (2014).

75. M. L. Bouxsein *et al.*, Guidelines for assessment of bone microstructure in rodents using micro-computed tomography. *J Bone Miner Res* **25**, 1468-1486 (2010).

76. A. M. Parfitt *et al.*, Bone histomorphometry: standardization of nomenclature, symbols, and units. Report of the ASBMR Histomorphometry Nomenclature Committee. *J Bone Miner Res* **2**, 595-610 (1987).

77. B. Schmid, C. Helfrich-Forster, T. Yoshii, A new ImageJ plug-in "ActogramJ" for chronobiological analyses. *J Biol Rhythms* **26**, 464-467 (2011).

78. C. Bingham, B. Arbogast, G. C. Guillaume, J. K. Lee, F. Halberg, Inferential statistical methods for estimating and comparing cosinor parameters. *Chronobiologia* **9**, 397-439 (1982).

79. R. Refinetti, G. C. Lissen, F. Halberg, Procedures for numerical analysis of circadian rhythms. *Biol Rhythm Res* **38**, 275-325 (2007).

80. S. N. Peirson, L. A. Brown, C. A. Pothecary, L. A. Benson, A. S. Fisk, Light and the laboratory mouse. *J Neurosci Methods* **300**, 26-36 (2018).

Figures and Tables

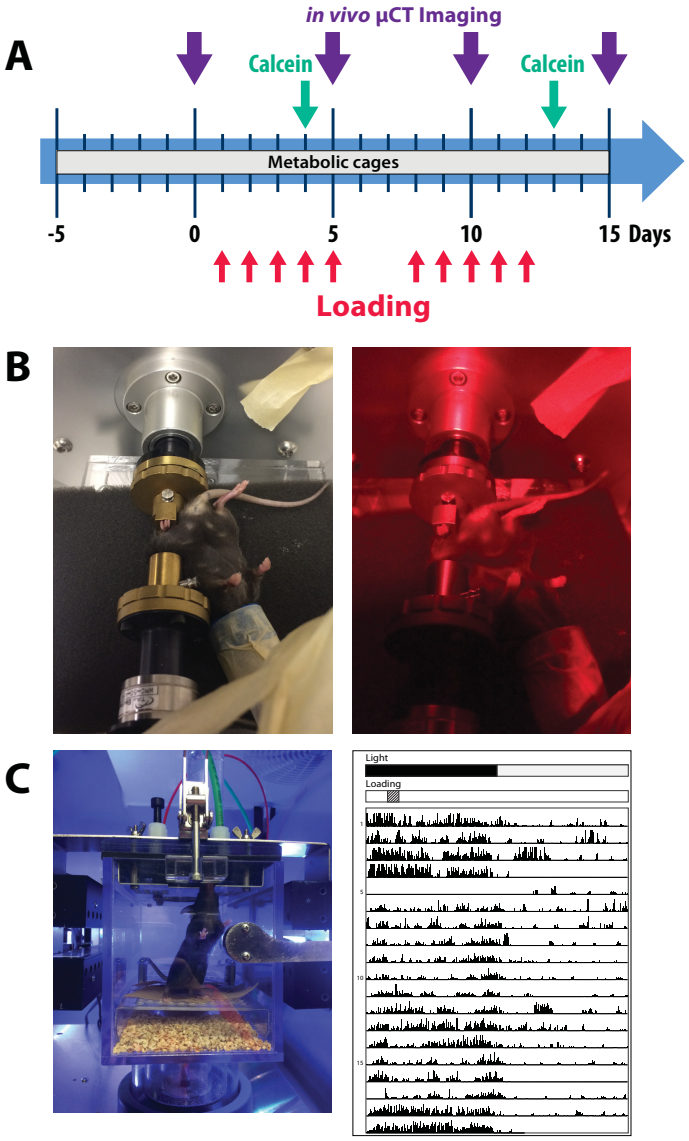

Figure 1. Experimental Design **A.** Experimental timeline. 10-week-old female C57Bl6/J mice underwent two weeks of in vivo loading (Monday-Friday) performed once per day. In vivo microCT was performed every 5 days throughout the experiment (day 0, 5, 10, 15), beginning one day prior to mechanical loading. Calcein was injected intraperitoneally 2 and 11 days prior to sacrifice. Mice were housed individually in metabolic cages for 20 days (day -5 until day 15) to measure activity. **B.** In vivo loading was performed either at ZT2(8:00am) or ZT14(8:00pm). Mice loaded at ZT14 were handled in dim red light during the dark phase to avoid disrupting their circadian rhythm as recommended (Peirson, Brown, Pothecary, Benson, & Fisk, 2018). **C.** Mouse inside metabolic cage and representative actogram of background activity data collected from these cages over the course of the experiment.

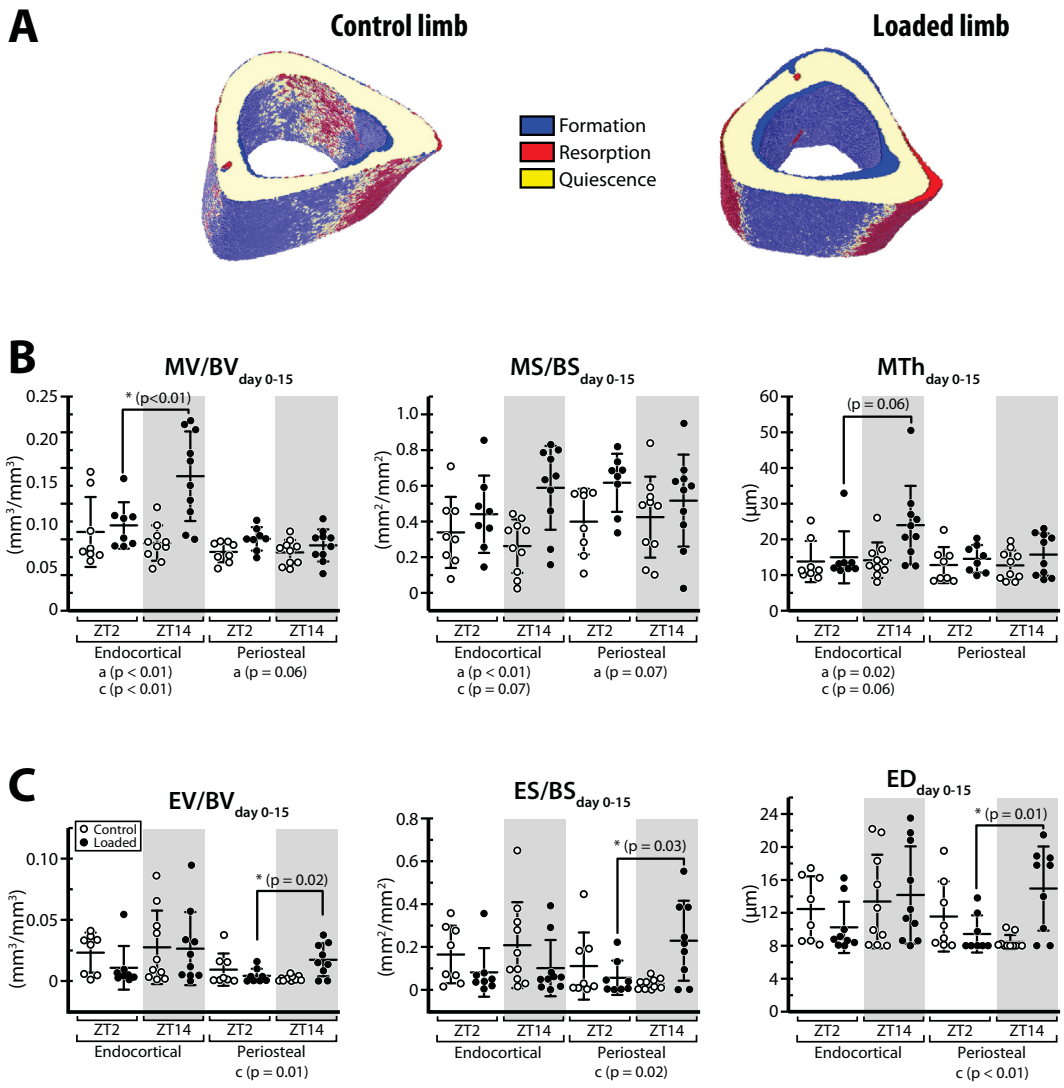

Figure 2. 3D registered microCT-based time-lapse morphometry of cortical bone at the tibial mid-shaft (Mean ± SD**). A.** Visualization of cortical bone (re)modeling occurring over the 15 day experimental period of left loaded tibia and right control tibia. The newly formed (blue), resorbed (red), and quiescent (yellow) bone can be seen on the endocortical and periosteal bone surface. **B.** Newly mineralizing volume fraction (MV/BV), mineralizing bone surface (MS/BS), and mineralizing thickness (MTh) of endocortical and periosteal bone. **C.** Newly eroding volume

fraction (EV/BV), eroding bone surface (ES/BS), and erosion depth (ED) of endocortical and periosteal bone. ANOVA main effects: (a) Loading; (b) Zeitgeber Time; (c) Interaction, followed by Tukey-Kramer post-hoc test: (*) $p < 0.05$.

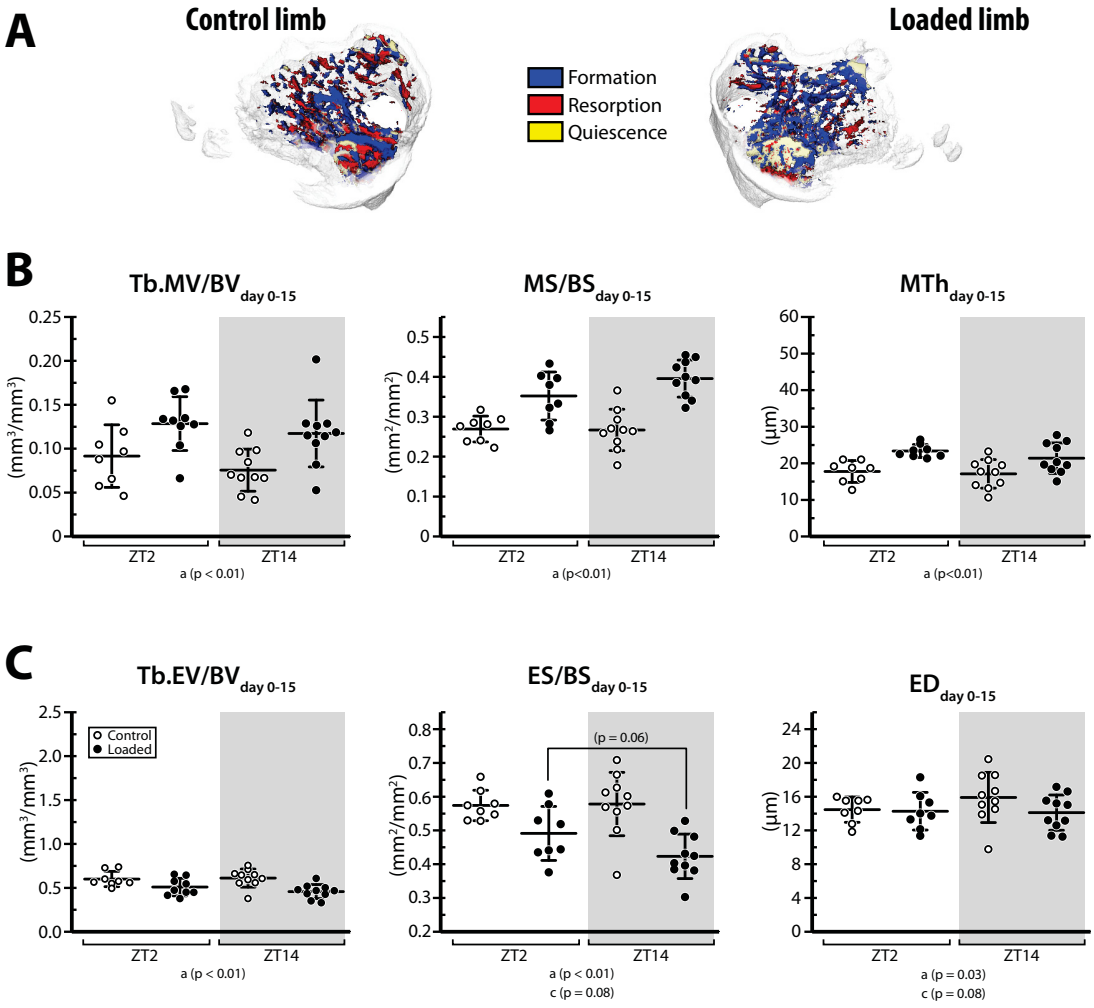

Figure 3. 3D registered microCT-based time-lapse morphometry of trabecular bone at the proximal tibial metaphysis (Mean ± SD). **A.** Visualization of trabecular bone (re)modeling occurring over the 15 day experimental period of left loaded tibia and right control tibia. The newly formed (blue), resorbed (red), and quiescent (yellow) bone can be seen on the trabecular bone surface. **B.** Newly mineralizing trabecular bone volume fraction (Tb. MV/BV), mineralizing bone surface (MS/BS), and mineralizing thickness (MTh). **C.** Newly eroding trabecular bone volume fraction (Tb.EV/BV), eroding bone surface (Es/BS), and erosion depth

(ED). ANOVA main effects: (a) Loading; (b) Zeitgeber Time; (c) Interaction $p < 0.05$. Tukey-Kramer post-hoc test (*) $p < 0.05$

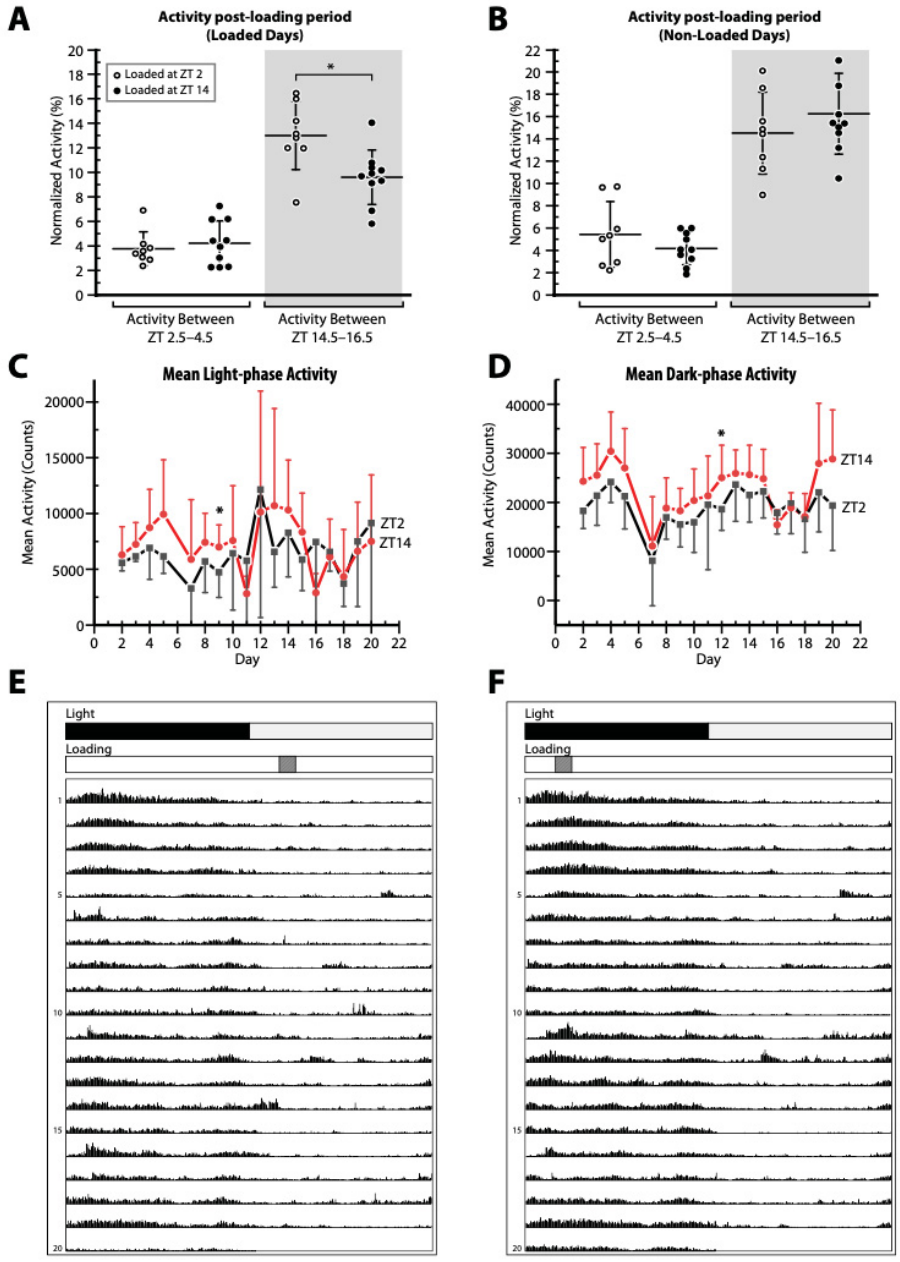

Figure 4. Differences in activity profiles between ZT2 and ZT14 mice. **A.** Activity recorded for 2 hours post-loading at ZT2.5 to ZT4.5 on loaded days (days 6,7,13,14) **B.** Activity recorded for 2 hours at ZT2.5 to ZT4.5 on non-loaded days (days 11,12,18,19). **C.** Mean light-phase activity in ZT2 vs ZT14 mice over the course of the experiment (day 1-20). **D.** Mean dark-phase activity in ZT2 vs ZT14 mice over the course of the experiment (day 1-20). **E.** A representative actogram

for a mouse loaded at ZT2, which shows mean activity over the course of the experiment (day 1-20). **F.** A representative actogram for a mouse loaded at ZT14, which shows mean activity over the course of the experiment (day 1-20). One-way ANOVA (*) – Zeitgeber Time

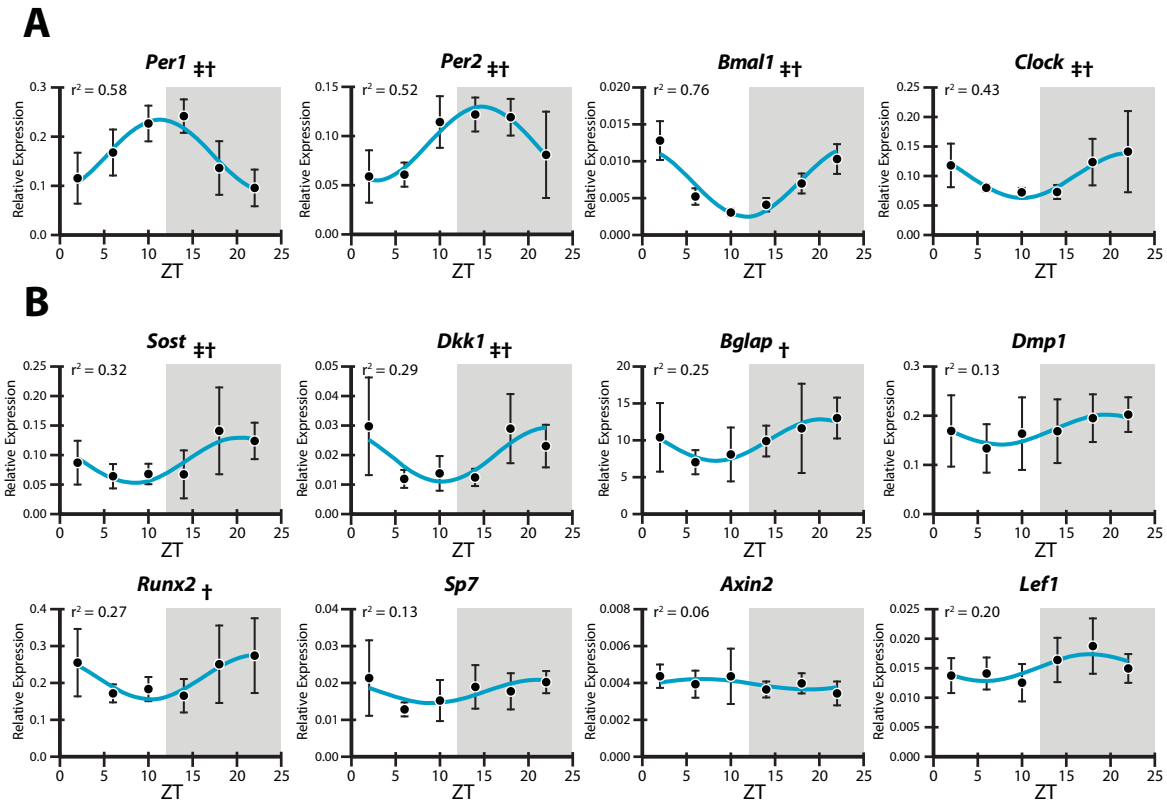

Figure 5. Relative gene expression in sham-loaded tibia of mice. **A.** Rhythmic core molecular clock gene expression in sham loaded tibial cortical bone (*Per1, Per2, Bmal1, Clock*). **B.** Rhythmic profile in osteocyte-specific and osteoblast-specific genes in sham tibial loaded cortical bone (*Sost, Dkk1, Bglap, Dmp1, Runx2, Sp7, Axin2, Lef1*). One-way ANOVA ǂ : Zeitgeber Time $p < 0.05$. Cosinor analysis † : 24-hour rhythmicity $p < 0.05$.

Figure 6. Serum bone turnover marker concentration of sclerostin, P1NP, and TRAP5b in sham-loaded tibia of mice. One-way ANOVA ǂ : Zeitgeber Time $p < 0.05$. Cosinor analysis † : 24-hour rhythmicity $p < 0.05$.

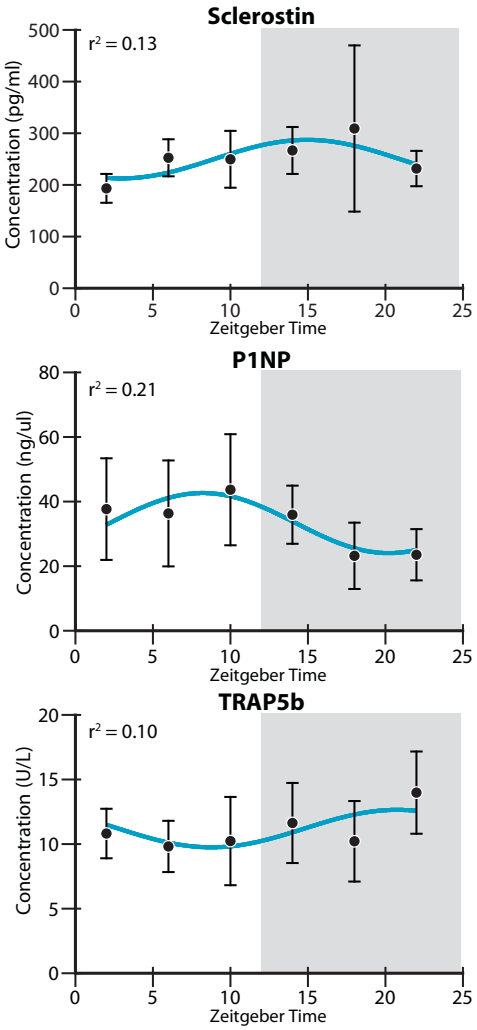

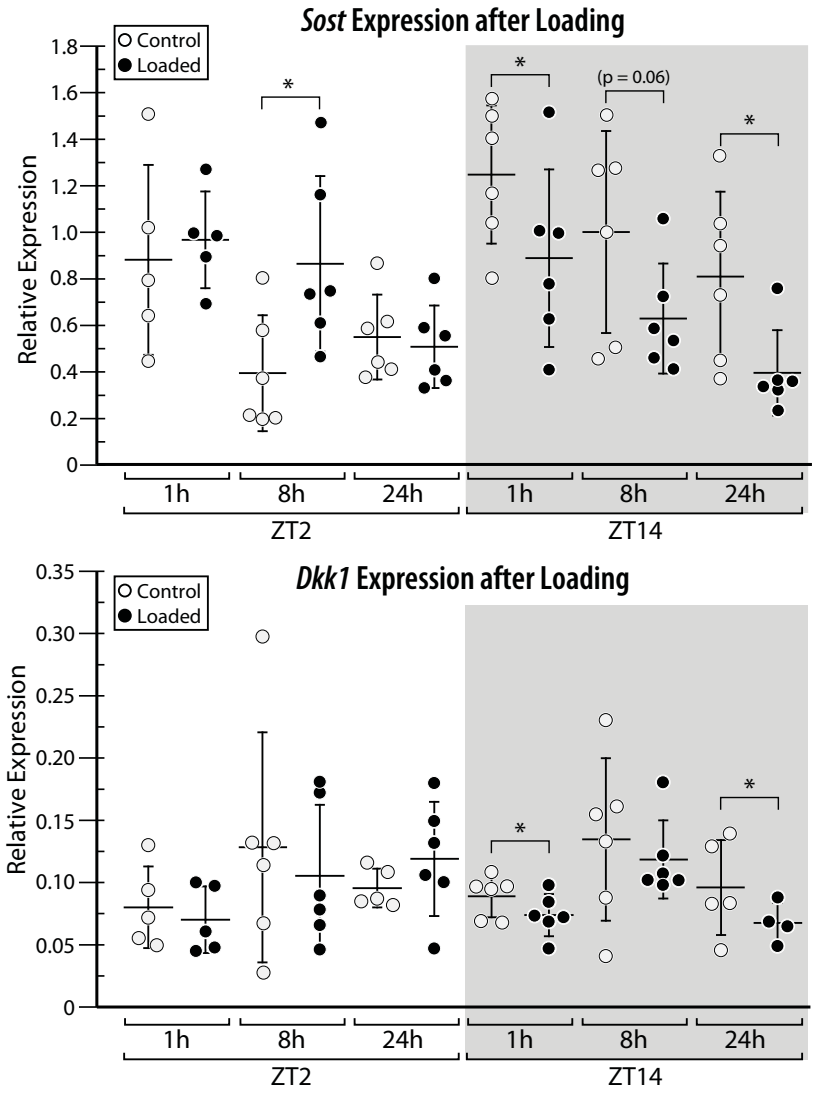

Figure 7. Relative *Sost* and *Dkk1* expression, 1h, 8h, and 24h after loading at either ZT2 or ZT14 in nonloaded control (right limb) tibiae and loaded (left limb) tibiae. Paired t-test (*) $p < 0.05$.

	ZT2		ZT14	
	Control	Loaded	Control	Loaded
Cortical Diaphysis				
Day 0-15	(n=8)	(n=8)	(n=10)	(n=10)
Ec.MV/BV [mm^3/mm^3][a,c,*]	0.06 ± 0.04	0.07 ± 0.03	0.04 ± 0.02	0.14 ± 0.06
Ec.MS/BS [mm^2/mm^2][a]	0.34 ± 0.20	0.46 ± 0.21	0.26 ± 0.15	0.59 ± 0.23
Ec.MTh [µm][a]	13.79 ± 5.78	14.75 ± 6.85	14.14 ± 4.98	23.98 ± 10.99
Ec.EV/BV [mm^3/mm^3]	0.02 ± 0.02	0.01 ± 0.02	0.03 ± 0.03	0.03 ± 0.03
Ec.ES/BS [mm^2/mm^2]	0.16 ± 0.13	0.07 ± 0.11	0.21 ± 0.20	0.10 ± 0.13
Ec.ED [µm]	12.47 ± 3.97	10.24 ± 3.11	13.37 ± 5.68	14.16 ± 5.91
Ps.MV/BV [mm^3/mm^3]	0.03 ± 0.01	0.05 ± 0.02	0.03 ± 0.02	0.04 ± 0.02
Ps.MS/BS [mm^2/mm^2]	0.40 ± 0.18	0.63 ± 0.16	0.42 ± 0.23	0.52 ± 0.26
Ps.MTh [µm]	12.79 ± 5.04	14.22 ± 3.73	12.70 ± 4.22	15.71 ± 5.90
Ps.EV/BV [mm^3/mm^3][c,*]	0.01 ± 0.01	0.004 ± 0.01	0.002 ± 0.002	0.02 ± 0.01
Ps.ES/BS [mm^2/mm^2][c,*]	0.11 ± 0.16	0.06 ± 0.08	0.03 ± 0.03	0.23 ± 0.19
Ps.ED [µm][c,*]	11.56 ± 4.26	9.44 ± 2.26	8.45 ± 0.86	14.96 ± 5.11
Cortical Metaphysis				
Day 0-15	(n=8)	(n=8)	(n=10)	(n=10)
Ec.MV/BV [mm^3/mm^3][a]	0.27 ± 0.07	0.35 ± 0.10	0.27 ± 0.08	0.34 ± 0.11
Ec.MS/BS [mm^2/mm^2]	0.70 ± 0.07	0.67 ± 0.07	0.66 ± 0.11	0.67 ± 0.10
Ec.EV/BV [mm^3/mm^3]	0.05 ± 0.03	0.04 ± 0.02	0.06 ± 0.02	0.04 ± 0.02
Ec.ES/BS [mm^2/mm^2]	0.13 ± 0.05	0.14 ± 0.06	0.15 ± 0.06	0.13 ± 0.05
Ec.MTh [µm][a]	29.90 ± 5.33	26.48 ± 3.86	31.32 ± 7.24	26.95 ± 5.03
Ec.ED [µm]	13.15 ± 2.46	14.11 ± 3.18	14.45 ± 1.86	12.50 ± 2.61
Ps.MV/BV [mm^3/mm^3][a]	0.02 ± 0.01	0.06 ± 0.02	0.03 ± 0.01	0.05 ± 0.02
Ps.MS/BS [mm^2/mm^2][a]	0.27 ± 0.13	0.62 ± 0.08	0.32 ± 0.16	0.54 ± 0.22
Ps.EV/BV [mm^3/mm^3][a]	0.04 ± 0.02	0.01 ± 0.01	0.04 ± 0.02	0.02 ± 0.01
Ps.ES/BS [mm^2/mm^2][a]	0.38 ± 0.17	0.15 ± 0.05	0.39 ± 0.16	0.20 ± 0.13
Ps.MTh [µm][a]	12.26 ± 2.30	16.90 ± 2.06	12.71 ± 2.60	15.58 ± 2.53
Ps.ED [µm]	13.98 ± 3.56	12.86 ± 2.59	14.53 ± 2.68	12.01 ± 2.02
Trabecular Metaphysis				
Day 0-15	(n=8)	(n=8)	(n=10)	(n=10)
Tb.MV/BV [mm^3/mm^3][a]	0.92 ± 0.36	1.28 ± 0.31	0.76 ± 0.24	1.17 ± 0.38
Tb.MS/BS [mm^2/mm^2][a]	0.27 ± 0.03	0.35 ± 0.06	0.27 ± 0.05	0.40 ± 0.05
Tb.EV/BV [mm^3/mm^3][a]	0.60 ± 0.09	0.52 ± 0.10	0.61 ± 0.10	0.46 ± 0.08
Tb.ES/BS [mm^2/mm^2][a]	0.57 ± 0.04	0.49 ± 0.08	0.58 ± 0.09	0.42 ± 0.07
Tb.MTh [µm][a]	17.76 ± 2.98	23.37 ± 1.77	17.11 ± 3.90	21.39 ± 4.18
Tb.ED [µm][a]	14.46 ± 1.50	14.27 ± 2.23	15.90 ± 2.97	14.11 ± 2.09

Table 1. 3D registered microCT-based time-lapse morphometry. Table depicts diaphyseal and metaphyseal cortical bone formation and resorption on the endocortical and periosteal surfaces (Day 0-15) in both loaded and control limbs of ZT2 and ZT14 mice. Table also depicts metaphyseal trabecular bone formation and resorption in both loaded and control limbs of ZT2 and ZT14 mice. Data presented as mean ± standard deviation. **ANOVA main effects**: (a)

Loading; (b) Zeitgeber Time; (c) Interaction, followed by **Tukey-Kramer post-hoc test: (*)** $p < 0.05$

Gene	Catalog Number
Per1	Mm00501813_m1
Per2	Mm00478099_m1
Arntl1 (Bmal1)	Mm00500226_m1
Clock	Mm00455950_m1
Sost	Mm00470479_m1
Dkk1	Mm00438422_m1
Bglap	Mm03413826_mH
Dmp1	Mm01208363_m1
Runx2	Mm00501584_m1
Sp7	Mm04933803_m1
Axin2	Mm00443610_m1
Lef1	Mm00550265_m1

Table 2. List of qPCR Probes used in the study along with the Thermo-Fisher catalog numbers.

Supplementary Results

Loading led to a robust cortical and trabecular bone formation response at the metaphyseal region

We observed load-induced cortical bone formation at the metaphyseal region. 3D registered time-lapse morphometry revealed significantly greater bone formation ($Ps.MV/BV_{day0-15}$: 158%, $Ps.MS/BS_{day0-15}$: 143%, $Ps.MTh_{day0-15}$: 33%, $Ec.MV/BV_{day0-15}$: 32%) and lower bone resorption ($Ps.EV/BV_{day0-15}$: -52%, $Ps.ES/BS_{day0-15}$: -52%, $Ps.ED_{day0-15}$: -10%) in loaded compared to control limbs (Table 1). The bone formation response to loading was greater in the diaphyseal region (185% increase in $Ec.MV/BV_{day0-15}$ in loaded vs control limbs) compared to the metaphyseal region (32% increase in $Ec.MV/BV_{day0-15}$ in loaded vs control limbs).

At day 15, all microCT outcome parameters (Imax: 29%, Imin: 38%, Ct.Ar: 21%, Tt.Ar: 21%, Ct.Ar/Tt.Ar: 0.5%, Ct.Th: 13%, and Ct.vTMD: 2.3%) were greater in the loaded compared to control limbs. The Ct.Th, and Ma.Ar were significantly different in loaded and control limbs at day 0. When analyzing change from baseline, we observed a significantly greater ΔCt.Ar, ΔCt.Ar/Tt.Ar, ΔTt.Ar, ΔCt.Th, ΔMa.Ar ΔCt.TMD, ΔImax, and ΔImin in the loaded compared to the control limb (Supplemental fig. 1). Conventional histomorphometry was not measured in this region.

Finally in the trabecular bone compartment of the proximal metaphysis, 3D registered time-lapse morphometry confirmed significantly greater trabecular bone formation ($Tb.MV/BV_{day0-15}$: 56%, $Tb.MS/BS_{day0-15}$: 43%, $Tb.MTh_{day0-15}$: 30%) and lower resorption ($Tb.EV/BV_{day0-15}$: -18%), $Tb.ES/BS_{day0-15:}$ -21%, $Tb.ED_{day0-15}$: -6%) due to loading (Fig. 2; Table 1).

At day 15, we also observed significantly greater microCT parameters (Tb.BV/TV: 124%, Tb.Th: 29%, Tb.N: 74%, Tb.vTMD: 9%) as well as significantly lower Tb.Sp: -6% at day 15 in loaded compared to control limbs. The TbTh was significantly different in loaded and control limbs at day 0. We measured a significantly greater ΔTb.BV/TV, ΔTb.BS/BV, ΔTb.Th, ΔTb.N, and ΔTb.vTMD in the loaded compared to the control limb (Supplemental fig. 1). Histomorphometry of trabecular bone revealed no significant differences due to loading.

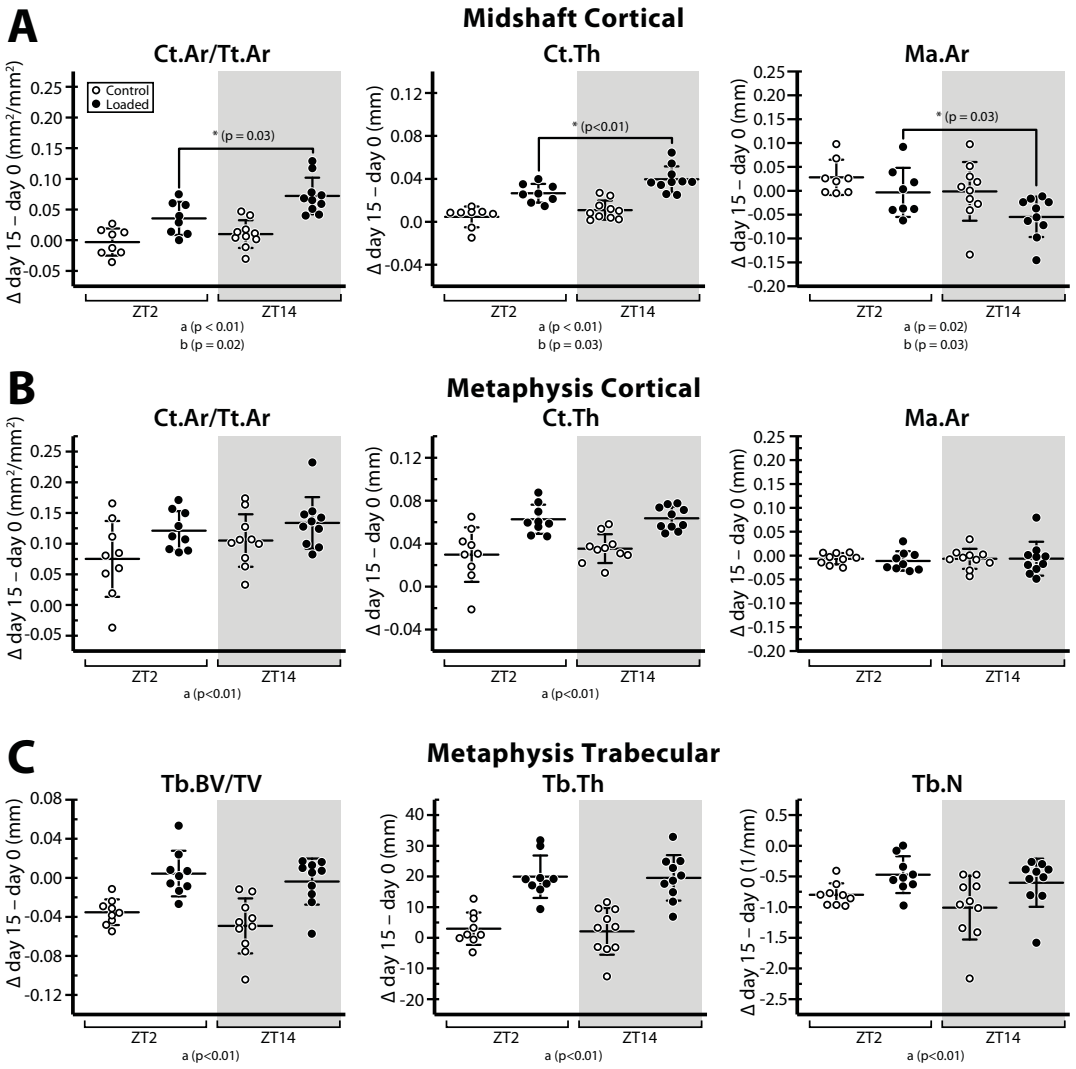

Supplemental Figure 1. Conventional unregistered microCT analysis of three volumes of interest, showing change from baseline (day15 - day0) (Mean ± SD). **A.** Midshaft cortical bone cortical area fraction (Ct.Ar/Tt.Ar), cortical thickness (Ct.Th), and marrow area (Ma.Ar) **B.** Proximal metaphysis cortical bone cortical area fraction (Ct.Ar/Tt.Ar), cortical thickness (Ct.Th), and marrow area (Ma.Ar) **C.** Proximal metaphysis trabecular bone volume fraction (Tb.BV/TV), trabecular thickness (Tb.Th), and trabecular number (Tb.N). ANOVA main effects: (a) Loading; (b) Zeitgeber Time; (c) Interaction, followed by Tukey-Kramer post-hoc test: (*) $p < 0.05$.

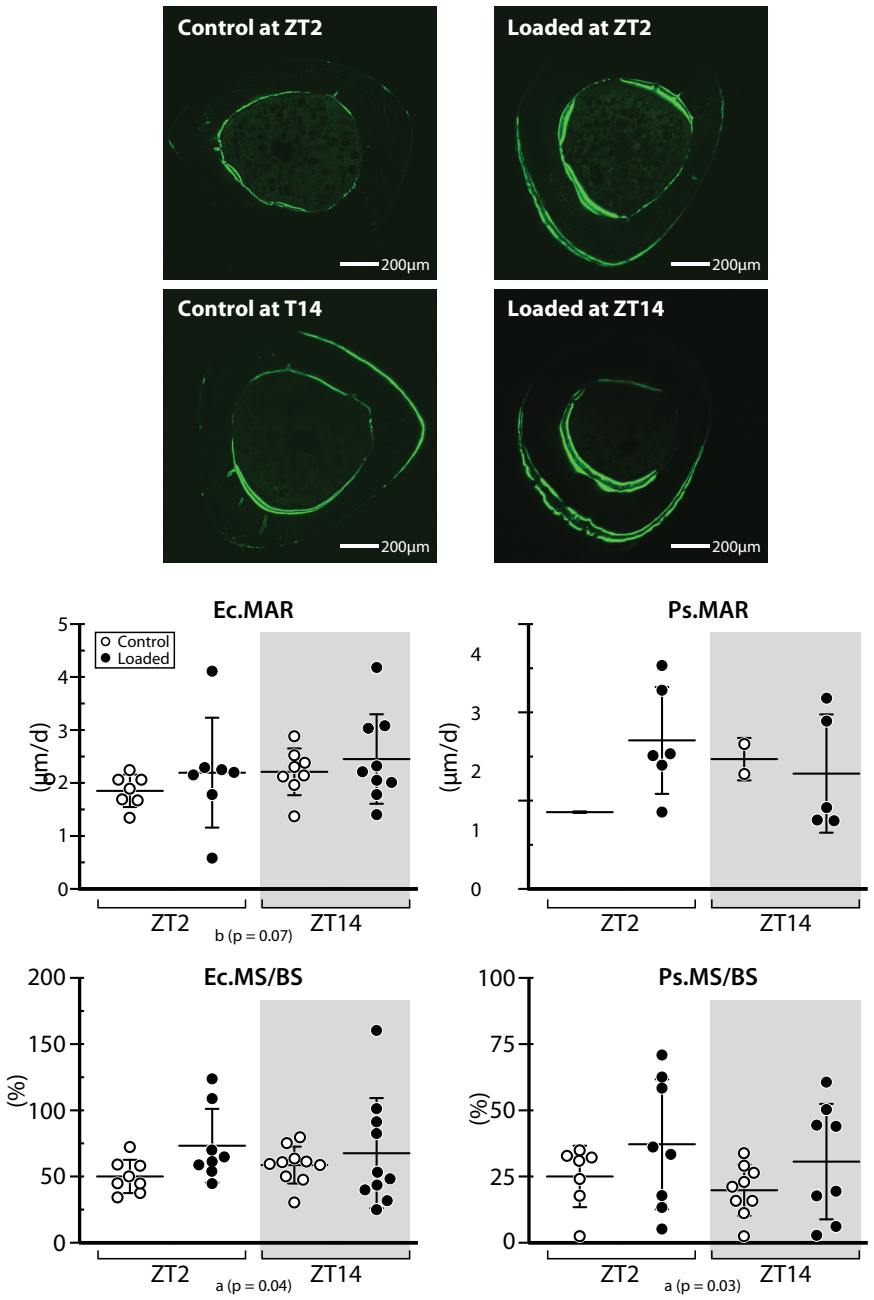

Supplemental Figure 2. Conventional histomorphometry in mid-diaphyseal cortical bone. **A.** Images of transverse sections of the mid-diaphysis from the loaded limb and control limb of mice loaded at ZT2 or ZT14, showing calcein double labeling, administered 11 and 2 days prior to sacrifice. **B.** Endocortical (Ec.) and periosteal (Ps.) mineral apposition rates (MAR) and

mineralizing surface normalized to bone surface (MS/BS). ANOVA main effects: (a) Loading; (b) Zeitgeber Time; (c) Interaction $p < 0.05$. Tukey-kramer Post-hoc test pairwise comparison tests: (*) $p < 0.05$.

	ZT 2		ZT 14	
	control	loaded	control	loaded
Day 15	(n=8)	(n=8)	(n=9)	(n=9)
Tb.MS/BS (%)	26.1 ± 4.4	60.5 ± 3.2	28.3 ± 5.1	27.4 ± 4.7
Tb.MAR (μm/day)	2.48 ± 0.29	2.26 ± 0.41	2.58 ± 0.57	2.38 ± 0.36
Tb.BFR (μm/day)	0.67 ± 0.18	0.69 ± 0.16	0.71 ± 0.19	0.64 ± 0.11
Tb.sLS/BS (%)	31.1 ± 11.3	33.9 ± 5.6	41.5 ± 13.8	27.9 ± 7.5
Tb.dLS/BS (%)	12.0 ± 8.3	13.5 ± 3.63	8.6 ± 7.2	13.6 ± 4.8

Supplemental Table 1. Conventional histomorphometry in trabecular bone. Table depicts dynamic histomorphometry measurements in both loaded and control limbs of ZT2 and ZT14 mice. The trabecular bone (Tb) at the proximal metaphysis was measured based on fluorochrome injections administered 2 and 11 days prior to euthanasia. Data presented as mean ± standard deviation. ANOVA main effects: (a) Loading; (b) Zeitgeber Time; (c) Interaction, followed by Tukey-Kramer post-hoc test: (*) $p < 0.05$.

Chapter 3: Extended Discussion

In previous experiments in our laboratory, we have shown through finite element modeling that the tibiae of mice undergoing mechanical loading through our protocol have high strains engendered at the 50% region (Razi et al., 2015). It has also been previously reported that bone formation occurs preferentially at areas of higher strain, in other words locations where the strain surpasses the mechanostat setpoint, triggering bone formation (Frost, 1987). Therefore, we aimed to study the effects of mechanical loading of our mice in cortical bone at the 50% diaphyseal region and trabecular bone at the proximal tibia in the metaphyseal region as previously done in our lab. We observed different responses between cortical and trabecular bone. We show that cortical bone responds preferentially to mechanical loading at ZT14, compared to ZT2, and that this response corresponds to greater downregulation of *Sost* and *Dkk1* expression. We did not analyze trabecular bone gene expression. At the tissue level, unlike in the cortical bone, we did not observe any zeitgeber time dependent changes in trabecular bone formation. This disparity in tissue-level response may be due to unknown changes in gene expression between cortical and trabecular bone. Trabecular bone is known to express very different genes and serve various different roles than cortical bone (Li et al., 2017). Trabecular, or cancellous bone, serves as support for the cortical bone around it through its many interconnections, simultaneously reducing its weight (Burr, 2019). The space between trabecular bone allows for the production of blood, an essential function of bone. Cortical bone on the other hand provides skeletal structure and protection (Burr, 2019). Beyond different functions, cortical and cancellous bone exhibit different bone remodeling levels (Li et al., 2017). Therefore, it is unsurprising that our cortical and trabecular bone displayed different responses to mechanical loading. Perhaps the precise zeitgeber time of mechanical loading could be used to target these

different bone regions. Midshaft cortical bone responds preferentially to loading at ZT14 than ZT2, but perhaps trabecular bone in the metaphysis has a greater response at ZT17 (for example). Further studies examining the effect of mechanical loading at different zeitgeber times, and studies examining the gene expression profile in trabecular bone are necessary to completely understand the complicated effect of mechanical loading at different times of day.

In our experiments, we show that greater bone formation occurred in cortical bone when mice were loaded at ZT14 compared to ZT2. We observed that *Sost* expression was downregulated in the loaded limbs of ZT14 mice, but not in mice loaded at ZT2. We also observed that at ZT2, mice had less *Sost* expression than at ZT14 in sham-loaded mice. However, we also noticed that *Sost* expression had a peak at ZT18 and a trough of expression at ZT6. Based on this information, while our tissue-level experiment was able to quantify a difference between loading at ZT2 and ZT14, we may see greater differences at ZT6 and ZT18. Repeating our experiments at these times, we hypothesize that mechanical loading when *Sost* is highest – ZT18, would result in a greater downregulation of *Sost* expression than when *Sost* is lowest. In turn, this greater downregulation of *Sost* would result in less inhibition of the wnt signaling pathway. As a result, bones loaded at ZT18 may display greater bone formation than bones loaded at ZT6.

In addition to observing cyclic expression of *Sost,* we observed significant circadian rhythms in important clock genes *Bmal1, Clock, Per1,* and *Per2.* We observed that, as expected, *Bmal1* and *Clock* were expressed antiphase of *Per1* and *Per2.* We also noted that the phase of each gene's rhythm was consistent with other bone studies in the literature (Fu et al., 2005; Schilperoort et al., 2020; Takarada et al., 2017). This suggests that the circadian clock in bone is highly conserved.

Both our tissue-level and gene-level experiments were conducted on mice that were kept in a 12/12 light-dark cycle. This lighting scheme was chosen in order to mimic the normal environment, thus providing for slightly simpler translation into a clinical setting. However, running this experiment in these conditions may have masked some of the effects of loading on the circadian rhythm. For instance, it remains possible that mechanical loading at different times of day has the ability to phase-shift the circadian rhythm of our animals, although this was not observed in our study. It is also possible that loading changes the peripheral circadian rhythm in bone. It is well understood that light is a very significant zeitgeber, entraining the circadian rhythm of animals to their environment (Dibner et al., 2010). In the absence of light, less significant zeitgebers can be seen to have an effect on the circadian rhythm. To test if mechanical loading specifically has this zeitgeber ability, it would be necessary to repeat this experiment in the complete darkness, as opposed to the light/dark cycle we used, so that light cannot mask any potential effects.

In addition to light, physical activity can lead to phase-shifting effects on the circadian rhythm in muscle (G. Wolff & Esser, 2012), therefore we hypothesized that background activity may be important in the circadian clock of bone. Keeping this potential effect in mind, we recorded the activity of our mice by housing them in metabolic cages for the duration of our tissue-level experiment. We observed no phase-shifting, onset-offset, nor global changes in the activity of our mice between groups. In addition, we noted significant reductions in activity immediately post-loading in our ZT14 mice, the mice who generated more bone than their ZT2 counterparts. Therefore, we are confident our differences are not attributable to effects of activity as a zeitgeber.

Beyond the potential masking effect that light may have on our mice, simply our treatment may have changed the gene expression or serum protein expression of our mice. While our cyclic rhythm characterization of bone mRNA and serum proteins was performed on sham-loaded mice, even these mice were removed from their home cages and anesthetized for the duration of a loading cycle (approximately 5 minutes). Although we aimed to disrupt the circadian rhythm of these mice as little as possible, it remains a possibility that disrupting these mice 8 hours prior to sacrifice modified the gene or protein expression. However, as noted above, the phase of our clock gene mRNA was similar to those reported in previous studies (Fu et al., 2005; Schilperoort et al., 2020; Takarada et al., 2017), suggesting that any disruptions to the endogenous circadian rhythm were likely minimal.

We observed no significant circadian rhythm in serum samples of Sclerostin, P1NP, and TRAP5b. While it has not been shown that Sclerostin in serum exhibits a rhythm, there have been rhythms of P1NP previously observed in human serum samples (Fraser, Ahmad, & Vora, 2004; Redmond et al., 2016). Although we have not observed a significant rhythm, we do observe trends towards one ($p=0.07$) with a peak at ZT10 and trough at ZT18. In humans, serum P1NP has been expressed as rhythmic in studies will large sample sizes. Fraser et al. report that the rhythm of P1NP in humans appears to peak around ZT22 with a trough around ZT8 (Fraser et al., 2004). Redmond et al. report slightly different results with a peak around ZT18 and a trough ZT2 (Redmond et al., 2016). Despite the slight offset between these two human studies, it appears that these reported rhythms are anti-phase from ours, suggesting that bone turnover rhythms in mice are anti-phase from human rhythms. As mice are nocturnal, it has been assumed that translating our observed results into humans would involve inverting them. Since bone turnover appears to express an anti-phase rhythm in mice, it can be assumed that both our gene

expression and tissue level results, that *Sost* expression is diminished after loading at ZT14 and greater bone formation occurs in mice loaded at ZT14, should be inverted. Therefore, it may be beneficial for humans to perform loading or exercise regimes in the morning to best improve their bone health.

Our study has many strengths. My research is the first to examine tissue-level changes in bones subjected to in-vivo mechanical loading. In this experiment, we used a higher resolution scan (8μm) compared to the 10μm used in many previous studies. In addition, our scanning protocol subjected the mice to radiation levels (100-200mGy/scan) much lower than the levels shown to cause damage in mice of this age (0.48Gy/scan) (Klinck, Campbell, & Boyd, 2008; Willie et al., 2013). Beyond our state-of-the-art imaging protocol, we were also able to quantify changes in the global circadian rhythm of our mice by housing them in metabolic cages for the duration of the experiment. These cages allowed us to ensure the mice were not exposed to light at night. They also allowed us to quantify background loading during our study. As it has been shown that abnormal background loading may interfere with load-induced bone formation (Meakin et al., 2013), this equipment allowed us to ensure that there were no differences between our ZT2 and ZT14 mice. In parallel, we examined the gene-expression changes that resulted from a single bout of *in-vivo* mechanical loading. Our multiple dissection points allowed us to quantify early, middle, and late changes in gene expression after loading. We also maintained a group of sham-loaded mice, allowing us to measure the rhythmic expression of several clock genes, as well as some bone specific genes, in the absence of any potential systemic changes due to mechanical loading. To date, we are the first group to demonstrate significant rhythmicity in *Sost* and *Dkk1* expression in mouse tibiae.

Our study also had limitations. Our microCT imaging machine involves placing the mouse inside a cassette. To limit variability between scans and between mice, we custom designed and 3D printed a mouse bed. However, this bed was only used for a portion of the experiment (n=8 mice). In addition, slight tilting of the cassette may have resulted in a systematic error being introduced. Our microCT machine works best when a sample is placed precisely in the center of the field of view. Because of this offset, and since we scan both legs at once, there may be a discrepancy in our scans. Another limitation in *in-vivo* imaging is movement artifacts. Although we limited moment as much as possible, by modifying our anesthesia dosage and by generating a 3D printed bed, some scans still contained movement, reducing the clarity of our image. In addition, our 2-week loading study was conducted at 2 timepoints – ZT2 and ZT14. It remains likely that these timepoints are not the precise peak and trough in the circadian rhythm of bone. While they exhibit differences in *Sost* downregulation and in bone formation, further work is needed to properly elucidate the optimal time for treatment.

Future directions of this project are vast. As we showed that clock gene expression in cortical bone is robust and exhibits a circadian rhythm, and this population is primarily made up of osteocytes, we hope to generate conditional knockout animals, whose osteocytes lack *Bmal1.* In these knockouts, we would repeat both tissue-level and gene-level experiments. We believe that by knocking out the peripheral circadian clock in osteocytes, we may negate the differences between loading at different times of day. We may also observe that *Sost* and *Dkk1* rhythmicity disappears in these animals. Another future direction of this project would involve repeating our tissue-level experiment at different timepoints, for instance ZT6 and ZT18. In this experimental modification, we may be able to quantify greater differences in the cortical bone formation response to mechanical loading, amplifying the results seen in the present study.

Chapter 4: Conclusion and Summary

In this thesis, we aimed to determine if the zeitgeber time of loading influences the adaptive bone formation response and to determine if the zeitgeber time of loading affects osteoblast and osteocyte gene expression. We demonstrate herein the importance of the circadian rhythm of bone in the adaptive bone formation response generated by mechanical loading. We observed that mechanical loading at different times of day result in greater bone formation in mice loaded at ZT14 (8pm) than mice loaded at ZT2 (8am) in midshaft cortical bone, but not in metaphyseal cortical or trabecular bone. We observed that mechanical loading resulted in less background activity immediately after loading in ZT14 mice, and no overall differences in global background activity between ZT2 and ZT14 mice. As there was no increased background activity in our ZT14 mice, our differences in cortical bone formation between our mice can be solely attributed to differences in the circadian rhythm of bone at ZT2 and ZT14. In addition, we report the cyclic gene expression of both clock genes and bone-specific genes in cortical bone of sham-loaded mice. As a result of this oscillatory profile, we observed zeitgeber time dependent downregulation of *Sost* and *Dkk1* expression in loaded limbs. Mice that were loaded in the evening (ZT14) displayed a sustained downregulation of *Sost* and *Dkk1,* whereas mice loaded at ZT2 displayed increases in *Sost* expression. Finally, serum bone turnover markers did not exhibit any circadian variation in expression. Therefore, we suggest that loading at time points when *Sost* and *Dkk1* levels are naturally elevated, as a function of the circadian rhythm, results in greater downregulation of wnt signaling inhibitors*,* resulting in greater bone formation that occurs in a position-dependent manner.

This study may help patients with osteoporosis, bone fragility, external fixators, and even astronauts. In conditions where mechanical loading is essential and beneficial, targeting this

loading to the best time point in the circadian rhythm may help to generate the greatest bone formation or bone maintenance effect. However, further studies are warranted in order to translate our results into a human population.

In conclusion, the peripheral circadian rhythm of bone must be taken into account both in mechanical loading and gene expression studies. The cyclic variation in genes such as *Sost* and *Dkk1* suggest that care should be taken to always measure their levels at the same time of day. In addition, mechanical loading studies should be performed at the same zeitgeber time, in order to avoid variations in results as a function of the natural circadian rhythm. Finally, mechanical loading studies targeted specifically when *Sost* and *Dkk1* levels are higher may result in greater anabolic bone formation responses.

References

Albiol, L., Cilla, M., Pflanz, D., Kramer, I., Kneissel, M., Duda, G. N., . . . Checa, S. (2018). Sost deficiency leads to reduced mechanical strains at the tibia midshaft in strain-matched in vivo loading experiments in mice. *J R Soc Interface, 15*(141). doi:10.1098/rsif.2018.0012

Asher, G., & Schibler, U. (2011). Crosstalk between components of circadian and metabolic cycles in mammals. *Cell Metab, 13*(2), 125-137. doi:10.1016/j.cmet.2011.01.006

Baron, R., & Hesse, E. (2012). Update on bone anabolics in osteoporosis treatment: rationale, current status, and perspectives. *J Clin Endocrinol Metab, 97*(2), 311-325. doi:10.1210/jc.2011-2332

Baud, C. A. (1962). [Morphology and inframicroscopic structure of osteocytes]. *Acta Anat (Basel), 51*, 209-225. Retrieved from https://www.ncbi.nlm.nih.gov/pubmed/13966889

Beck, B. R., & Snow, C. M. (2003). Bone health across the lifespan--exercising our options. *Exerc Sport Sci Rev, 31*(3), 117-122. doi:10.1097/00003677-200307000-00003

Bellido, T., Ali, A. A., Gubrij, I., Plotkin, L. I., Fu, Q., O'Brien, C. A., . . . Jilka, R. L. (2005). Chronic elevation of parathyroid hormone in mice reduces expression of sclerostin by osteocytes: a novel mechanism for hormonal control of osteoblastogenesis. *Endocrinology, 146*(11), 4577-4583. doi:10.1210/en.2005-0239

Berman, A. G., Hinton, M. J., & Wallace, J. M. (2019). Treadmill running and targeted tibial loading differentially improve bone mass in mice. *Bone Rep, 10*, 100195. doi:10.1016/j.bonr.2019.100195

Bingham, C., Arbogast, B., Guillaume, G. C., Lee, J. K., & Halberg, F. (1982). Inferential statistical methods for estimating and comparing cosinor parameters. *Chronobiologia, 9*(4), 397-439. Retrieved from https://www.ncbi.nlm.nih.gov/pubmed/7168995

Birkhold, A. I., Razi, H., Duda, G. N., Checa, S., & Willie, B. M. (2017). Tomography-Based Quantification of Regional Differences in Cortical Bone Surface Remodeling and Mechano-Response. *Calcif Tissue Int, 100*(3), 255-270. doi:10.1007/s00223-016-0217-4

Birkhold, A. I., Razi, H., Duda, G. N., Weinkamer, R., Checa, S., & Willie, B. M. (2014a). The influence of age on adaptive bone formation and bone resorption. *Biomaterials, 35*(34), 9290-9301. doi:10.1016/j.biomaterials.2014.07.051

Birkhold, A. I., Razi, H., Duda, G. N., Weinkamer, R., Checa, S., & Willie, B. M. (2014b). Mineralizing surface is the main target of mechanical stimulation independent of age: 3D dynamic in vivo morphometry. *Bone, 66*, 15-25. doi:10.1016/j.bone.2014.05.013

Birkhold, A. I., Razi, H., Duda, G. N., Weinkamer, R., Checa, S., & Willie, B. M. (2016). The Periosteal Bone Surface is Less Mechano-Responsive than the Endocortical. *Sci Rep, 6*, 23480. doi:10.1038/srep23480

Bonewald, L. (2019). Use it or lose it to age: A review of bone and muscle communication. *Bone, 120*, 212-218. doi:10.1016/j.bone.2018.11.002

Bonewald, L. F., & Johnson, M. L. (2008). Osteocytes, mechanosensing and Wnt signaling. *Bone, 42*(4), 606-615. doi:10.1016/j.bone.2007.12.224

Bouxsein, M. L., Boyd, S. K., Christiansen, B. A., Guldberg, R. E., Jepsen, K. J., & Muller, R. (2010). Guidelines for assessment of bone microstructure in rodents using micro-computed tomography. *J Bone Miner Res, 25*(7), 1468-1486. doi:10.1002/jbmr.141

Braith, R. W., Conner, J. A., Fulton, M. N., Lisor, C. F., Casey, D. P., Howe, K. S., & Baz, M. A. (2007). Comparison of alendronate vs alendronate plus mechanical loading as prophylaxis for osteoporosis in lung transplant recipients: a pilot study. *J Heart Lung Transplant, 26*(2), 132-137. doi:10.1016/j.healun.2006.11.004

Brunkow, M. E., Gardner, J. C., Van Ness, J., Paeper, B. W., Kovacevich, B. R., Proll, S., . . . Mulligan, J. (2001). Bone dysplasia sclerosteosis results from loss of the SOST gene product, a novel cystine knot-containing protein. *Am J Hum Genet, 68*(3), 577-589. doi:10.1086/318811

Burr, D. (2019). *Basic and applied bone biology* (2nd edition. ed.). Waltham, MA: Elsevier.

Chang, J., Garva, R., Pickard, A., Yeung, C. C., Mallikarjun, V., Swift, J., . . . Kadler, K. E. (2020). Circadian control of the secretory pathway maintains collagen homeostasis. *Nat Cell Biol, 22*(1), 74-86. doi:10.1038/s41556-019-0441-z

Chermside-Scabbo, C. J., Harris, T. L., Brodt, M. D., Braenne, I., Zhang, B., Farber, C. R., & Silva, M. J. (2020). Old Mice Have Less Transcriptional Activation But Similar Periosteal Cell Proliferation Compared to Young-Adult Mice in Response to in vivo Mechanical Loading. *J Bone Miner Res, 35*(9), 1751-1764. doi:10.1002/jbmr.4031

Clarke, B. L., & Drake, M. T. (2013). Clinical utility of serum sclerostin measurements. *Bonekey Rep, 2*, 361. doi:10.1038/bonekey.2013.95

Dallas, S. L., Prideaux, M., & Bonewald, L. F. (2013). The osteocyte: an endocrine cell ... and more. *Endocr Rev, 34*(5), 658-690. doi:10.1210/er.2012-1026

Delgado-Calle, J., Sato, A. Y., & Bellido, T. (2017). Role and mechanism of action of sclerostin in bone. *Bone, 96*, 29-37. doi:10.1016/j.bone.2016.10.007

Dibner, C., Schibler, U., & Albrecht, U. (2010). The mammalian circadian timing system: organization and coordination of central and peripheral clocks. *Annu Rev Physiol, 72*, 517-549. doi:10.1146/annurev-physiol-021909-135821

Ducher, G., Tournaire, N., Meddahi-Pelle, A., Benhamou, C. L., & Courteix, D. (2006). Short-term and long-term site-specific effects of tennis playing on trabecular and cortical bone at the distal radius. *J Bone Miner Metab, 24*(6), 484-490. doi:10.1007/s00774-006-0710-3

Duguay, D., & Cermakian, N. (2009). The crosstalk between physiology and circadian clock proteins. *Chronobiol Int, 26*(8), 1479-1513. doi:10.3109/07420520903497575

Engelke, K., Kemmler, W., Lauber, D., Beeskow, C., Pintag, R., & Kalender, W. A. (2006). Exercise maintains bone density at spine and hip EFOPS: a 3-year longitudinal study in early postmenopausal women. *Osteoporos Int, 17*(1), 133-142. doi:10.1007/s00198-005-1938-9

Fahlgren, A., Yang, X., Ciani, C., Ryan, J. A., Kelly, N., Ko, F. C., . . . Bostrom, M. P. (2013). The effects of PTH, loading and surgical insult on cancellous bone at the bone-implant interface in the rabbit. *Bone, 52*(2), 718-724. doi:10.1016/j.bone.2012.05.005

Fraser, W. D., Ahmad, A. M., & Vora, J. P. (2004). The physiology of the circadian rhythm of parathyroid hormone and its potential as a treatment for osteoporosis. *Curr Opin Nephrol Hypertens, 13*(4), 437-444. doi:10.1097/01.mnh.0000133985.29880.34

Frost, H. M. (1987). Bone "mass" and the "mechanostat": a proposal. *Anat Rec, 219*(1), 1-9. doi:10.1002/ar.1092190104

Frost, H. M. (1994). Wolff's Law and bone's structural adaptations to mechanical usage: an overview for clinicians. *Angle Orthod, 64*(3), 175-188. doi:10.1043/0003-3219(1994)064<0175:WLABSA>2.0.CO;2

Fu, L., Patel, M. S., Bradley, A., Wagner, E. F., & Karsenty, G. (2005). The molecular clock mediates leptin-regulated bone formation. *Cell, 122*(5), 803-815. doi:10.1016/j.cell.2005.06.028

Fujihara, Y., Kondo, H., Noguchi, T., & Togari, A. (2014). Glucocorticoids mediate circadian timing in peripheral osteoclasts resulting in the circadian expression rhythm of osteoclast-related genes. *Bone, 61*, 1-9. doi:10.1016/j.bone.2013.12.026

Greenspan, S. L., Dresner-Pollak, R., Parker, R. A., London, D., & Ferguson, L. (1997). Diurnal variation of bone mineral turnover in elderly men and women. *Calcif Tissue Int, 60*(5), 419-423. doi:10.1007/s002239900256

Grosso, M. J., Courtland, H. W., Yang, X., Sutherland, J. P., Stoner, K., Nguyen, J., . . . Bostrom, M. P. (2015). Intermittent PTH administration and mechanical loading are anabolic for periprosthetic cancellous bone. *J Orthop Res, 33*(2), 163-173. doi:10.1002/jor.22748

Haapasalo, H., Kontulainen, S., Sievanen, H., Kannus, P., Jarvinen, M., & Vuori, I. (2000). Exercise-induced bone gain is due to enlargement in bone size without a change in volumetric bone density: a peripheral quantitative computed tomography study of the upper arms of male tennis players. *Bone, 27*(3), 351-357. doi:10.1016/s8756-3282(00)00331-8

Halleux, C., Kramer, I., Allard, C., & Kneissel, M. (2012). Isolation of mouse osteocytes using cell fractionation for gene expression analysis. *Methods Mol Biol, 816*, 55-66. doi:10.1007/978-1-61779-415-5_5

Hastings, M. (1998). The brain, circadian rhythms, and clock genes. *BMJ, 317*(7174), 1704-1707. Retrieved from http://www.ncbi.nlm.nih.gov/pubmed/9857134

Hastings, M. H., & Herzog, E. D. (2004). Clock genes, oscillators, and cellular networks in the suprachiasmatic nuclei. *J Biol Rhythms, 19*(5), 400-413. doi:10.1177/0748730404268786

Hernlund, E., Svedbom, A., Ivergard, M., Compston, J., Cooper, C., Stenmark, J., . . . Kanis, J. A. (2013). Osteoporosis in the European Union: medical management, epidemiology and economic burden. A report prepared in collaboration with the International Osteoporosis Foundation (IOF) and the European Federation of Pharmaceutical Industry Associations (EFPIA). *Arch Osteoporos, 8*, 136. doi:10.1007/s11657-013-0136-1

Hirai, T., Tanaka, K., & Togari, A. (2014). beta-adrenergic receptor signaling regulates Ptgs2 by driving circadian gene expression in osteoblasts. *J Cell Sci, 127*(Pt 17), 3711-3719. doi:10.1242/jcs.148148

Igarashi, K., Miyoshi, K., Shinoda, H., Saeki, S., & Mitani, H. (1998). Diurnal variation in tooth movement in response to orthodontic force in rats. *Am J Orthod Dentofacial Orthop, 114*(1), 8-14. doi:10.1016/s0889-5406(98)70231-8

Inaoka, T., Lean, J. M., Bessho, T., Chow, J. W., Mackay, A., Kokubo, T., & Chambers, T. J. (1995). Sequential analysis of gene expression after an osteogenic stimulus: c-fos expression is induced in osteocytes. *Biochem Biophys Res Commun, 217*(1), 264-270. doi:S0006-291X(85)72773-8 [pii]

10.1006/bbrc.1995.2773

Jilka, R. L. (2013). The relevance of mouse models for investigating age-related bone loss in humans. *J Gerontol A Biol Sci Med Sci, 68*(10), 1209-1217. doi:10.1093/gerona/glt046

Jones, H. H., Priest, J. D., Hayes, W. C., Tichenor, C. C., & Nagel, D. A. (1977). Humeral hypertrophy in response to exercise. *J Bone Joint Surg Am, 59*(2), 204-208. Retrieved from https://www.ncbi.nlm.nih.gov/pubmed/845205

Jubiz, W., Canterbury, J. M., Reiss, E., & Tyler, F. H. (1972). Circadian rhythm in serum parathyroid hormone concentration in human subjects: correlation with serum calcium, phosphate, albumin, and growth hormone levels. *J Clin Invest, 51*(8), 2040-2046. doi:10.1172/JCI107010

Kawai, M., Kinoshita, S., Shimba, S., Ozono, K., & Michigami, T. (2014). Sympathetic activation induces skeletal Fgf23 expression in a circadian rhythm-dependent manner. *J Biol Chem, 289*(3), 1457-1466. doi:10.1074/jbc.M113.500850

Keller, H., & Kneissel, M. (2005). SOST is a target gene for PTH in bone. *Bone, 37*(2), 148-158. doi:10.1016/j.bone.2005.03.018

Klein, D. C., Moore, R. Y., & Reppert, S. M. (1991). *Suprachiasmatic nucleus : the mind's clock*. New York: Oxford University Press.

Klinck, R. J., Campbell, G. M., & Boyd, S. K. (2008). Radiation effects on bone architecture in mice and rats resulting from in vivo micro-computed tomography scanning. *Med Eng Phys, 30*(7), 888-895. doi:10.1016/j.medengphy.2007.11.004

Kohrt, W. M., Snead, D. B., Slatopolsky, E., & Birge, S. J., Jr. (1995). Additive effects of weight-bearing exercise and estrogen on bone mineral density in older women. *J Bone Miner Res, 10*(9), 1303-1311. doi:10.1002/jbmr.5650100906

Komoto, S., Kondo, H., Fukuta, O., & Togari, A. (2012). Comparison of beta-adrenergic and glucocorticoid signaling on clock gene and osteoblast-related gene expressions in human osteoblast. *Chronobiol Int, 29*(1), 66-74. doi:10.3109/07420528.2011.636496

Kontulainen, S., Sievanen, H., Kannus, P., Pasanen, M., & Vuori, I. (2003). Effect of long-term impact-loading on mass, size, and estimated strength of humerus and radius of female racquet-sports players: a peripheral quantitative computed tomography study between young and old starters and controls. *J Bone Miner Res, 18*(2), 352-359. doi:10.1359/jbmr.2003.18.2.352

Korpelainen, R., Keinanen-Kiukaanniemi, S., Heikkinen, J., Vaananen, K., & Korpelainen, J. (2006). Effect of impact exercise on bone mineral density in elderly women with low BMD: a population-based randomized controlled 30-month intervention. *Osteoporos Int, 17*(1), 109-118. doi:10.1007/s00198-005-1924-2

Kramer, I., Keller, H., Leupin, O., & Kneissel, M. (2010). Does osteocytic SOST suppression mediate PTH bone anabolism? *Trends Endocrinol Metab, 21*(4), 237-244. doi:10.1016/j.tem.2009.12.002

Kramer, I., Loots, G. G., Studer, A., Keller, H., & Kneissel, M. (2010). Parathyroid hormone (PTH)-induced bone gain is blunted in SOST overexpressing and deficient mice. *J Bone Miner Res, 25*(2), 178-189. doi:10.1359/jbmr.090730

Kunimoto, T., Okubo, N., Minami, Y., Fujiwara, H., Hosokawa, T., Asada, M., . . . Yagita, K. (2016). A PTH-responsive circadian clock operates in ex vivo mouse femur fracture healing site. *Sci Rep, 6*, 22409. doi:10.1038/srep22409

Lan, S., Luo, S., Huh, B. K., Chandra, A., Altman, A. R., Qin, L., & Liu, X. S. (2013). 3D image registration is critical to ensure accurate detection of longitudinal changes in trabecular bone density, microstructure, and stiffness measurements in rat tibiae by in vivo microcomputed tomography (muCT). *Bone, 56*(1), 83-90. doi:10.1016/j.bone.2013.05.014

Lang, T., LeBlanc, A., Evans, H., Lu, Y., Genant, H., & Yu, A. (2004). Cortical and trabecular bone mineral loss from the spine and hip in long-duration spaceflight. *J Bone Miner Res, 19*(6), 1006-1012. doi:10.1359/JBMR.040307

Leblanc, A., Matsumoto, T., Jones, J., Shapiro, J., Lang, T., Shackelford, L., . . . Ohshima, H. (2013). Bisphosphonates as a supplement to exercise to protect bone during long-duration spaceflight. *Osteoporos Int, 24*(7), 2105-2114. doi:10.1007/s00198-012-2243-z

Li, J., Bao, Q., Chen, S., Liu, H., Feng, J., Qin, H., . . . Zong, Z. (2017). Different bone remodeling levels of trabecular and cortical bone in response to changes in Wnt/beta-catenin signaling in mice. *J Orthop Res, 35*(4), 812-819. doi:10.1002/jor.23339

Li, J., Duncan, R. L., Burr, D. B., Gattone, V. H., & Turner, C. H. (2003). Parathyroid hormone enhances mechanically induced bone formation, possibly involving L-type voltage-sensitive calcium channels. *Endocrinology, 144*(4), 1226-1233. doi:10.1210/en.2002-220821

Luchavova, M., Zikan, V., Michalska, D., Raska, I., Jr., Kubena, A. A., & Stepan, J. J. (2011). The effect of timing of teriparatide treatment on the circadian rhythm of bone turnover in postmenopausal osteoporosis. *Eur J Endocrinol, 164*(4), 643-648. doi:10.1530/EJE-10-1108

Main, R. P., Shefelbine, S. J., Meakin, L. B., Silva, M. J., van der Meulen, M. C. H., & Willie, B. M. (2020). Murine Axial Compression Tibial Loading Model to Study Bone Mechanobiology: Implementing the Model and Reporting Results. *J Orthop Res, 38*(2), 233-252. doi:10.1002/jor.24466

Maronde, E., Schilling, A. F., Seitz, S., Schinke, T., Schmutz, I., van der Horst, G., . . . Albrecht, U. (2010). The clock genes Period 2 and Cryptochrome 2 differentially balance bone formation. *PLoS One, 5*(7), e11527. doi:10.1371/journal.pone.0011527

McElderry, J. D., Zhao, G., Khmaladze, A., Wilson, C. G., Franceschi, R. T., & Morris, M. D. (2013). Tracking circadian rhythms of bone mineral deposition in murine calvarial organ cultures. *J Bone Miner Res, 28*(8), 1846-1854. doi:10.1002/jbmr.1924

Meakin, L. B., Sugiyama, T., Galea, G. L., Browne, W. J., Lanyon, L. E., & Price, J. S. (2013). Male mice housed in groups engage in frequent fighting and show a lower response to additional bone loading than females or individually housed males that do not fight. *Bone, 54*(1), 113-117. doi:10.1016/j.bone.2013.01.029

Michalska, D., Luchavova, M., Zikan, V., Raska, I., Jr., Kubena, A. A., & Stepan, J. J. (2012). Effects of morning vs. evening teriparatide injection on bone mineral density and bone turnover markers in postmenopausal osteoporosis. *Osteoporos Int, 23*(12), 2885-2891. doi:10.1007/s00198-012-1955-4

Miyoshi, K., Igarashi, K., Saeki, S., Shinoda, H., & Mitani, H. (2001). Tooth movement and changes in periodontal tissue in response to orthodontic force in rats vary depending on the time of day the force is applied. *Eur J Orthod, 23*(4), 329-338. doi:10.1093/ejo/23.4.329

Moustafa, A., Sugiyama, T., Prasad, J., Zaman, G., Gross, T. S., Lanyon, L. E., & Price, J. S. (2012). Mechanical loading-related changes in osteocyte sclerostin expression in mice are more closely associated with the subsequent osteogenic response than the peak strains engendered. *Osteoporos Int, 23*, 1225–1234.

National Osteoporosis Foundation. Retrieved from nof.org

Oudet, C., Petrovic, A., & Stutzmann, J. (1984). Time-dependent effects of a 'functional'-type orthopedic appliance on the rat mandible growth. *Chronobiol Int, 1*(1), 51-57. Retrieved from https://www.ncbi.nlm.nih.gov/pubmed/6600009

Parfitt, A. M. (1994). Osteonal and hemi-osteonal remodeling: the spatial and temporal framework for signal traffic in adult human bone. *J Cell Biochem, 55*(3), 273-286. doi:10.1002/jcb.240550303

Parfitt, A. M. (2013). Skeletal Heterogeneity and the Purposes of Bone Remodeling: Implications for the Understanding of Osteoporosis. In D. F. Robert Marcus, David W. Dempster, Majorie Luckey, Jane A. Cauley (Ed.), *Osteoporosis (Forth Edition)* (pp. 855-872): Academic Press.

Parfitt, A. M., Drezner, M. K., Glorieux, F. H., Kanis, J. A., Malluche, H., Meunier, P. J., . . . Recker, R. R. (1987). Bone histomorphometry: standardization of nomenclature, symbols, and units. Report of the ASBMR Histomorphometry Nomenclature Committee. *J Bone Miner Res, 2*(6), 595-610. doi:10.1002/jbmr.5650020617

Patel, T. K., Brodt, M. D., & Silva, M. J. (2014). Experimental and finite element analysis of strains induced by axial tibial compression in young-adult and old female C57Bl/6 mice. *J Biomech, 47*(2), 451-457. doi:10.1016/j.jbiomech.2013.10.052

Peirson, S. N., Brown, L. A., Pothecary, C. A., Benson, L. A., & Fisk, A. S. (2018). Light and the laboratory mouse. *J Neurosci Methods, 300*, 26-36. doi:10.1016/j.jneumeth.2017.04.007

Pflanz, D., Birkhold, A. I., Albiol, L., Thiele, T., Julien, C., Seliger, A., . . . Willie, B. M. (2017). Sost deficiency led to a greater cortical bone formation response to mechanical loading and altered gene expression. *Sci Rep, 7*(1), 9435. doi:10.1038/s41598-017-09653-9

Piemontese, M., Almeida, M., Robling, A. G., Kim, H. N., Xiong, J., Thostenson, J. D., . . . Jilka, R. L. (2017). Old age causes de novo intracortical bone remodeling and porosity in mice. *JCI Insight, 2*(17). doi:10.1172/jci.insight.93771

Pivonka, P. (2018). *Multiscale Mechanobiology of Bone Remodeling and Adaptation*: Springer.

Qvist, P., Christgau, S., Pedersen, B. J., Schlemmer, A., & Christiansen, C. (2002). Circadian variation in the serum concentration of C-terminal telopeptide of type I collagen (serum CTx): effects of gender, age, menopausal status, posture, daylight, serum cortisol, and fasting. *Bone, 31*(1), 57-61. doi:10.1016/s8756-3282(02)00791-3

Razi, H., Birkhold, A. I., Zaslansky, P., Weinkamer, R., Duda, G. N., Willie, B. M., & Checa, S. (2015). Skeletal maturity leads to a reduction in the strain magnitudes induced within the bone: a murine tibia study. *Acta Biomater, 13*, 301-310. doi:10.1016/j.actbio.2014.11.021

Redmond, J., Fulford, A. J., Jarjou, L., Zhou, B., Prentice, A., & Schoenmakers, I. (2016). Diurnal Rhythms of Bone Turnover Markers in Three Ethnic Groups. *J Clin Endocrinol Metab, 101*(8), 3222-3230. doi:10.1210/jc.2016-1183

Refinetti, R., Lissen, G. C., & Halberg, F. (2007). Procedures for numerical analysis of circadian rhythms. *Biol Rhythm Res, 38*(4), 275-325. doi:10.1080/09291010600903692

Reppert, S. M., & Weaver, D. R. (2002). Coordination of circadian timing in mammals. *Nature, 418*(6901), 935-941. doi:10.1038/nature00965

Robling, A. G., Niziolek, P. J., Baldridge, L. A., Condon, K. W., Allen, M. R., Alam, I., . . . Turner, C. H. (2008). Mechanical stimulation of bone in vivo reduces osteocyte expression of Sost/sclerostin. *J Biol Chem, 283*(9), 5866-5875. doi:10.1074/jbc.M705092200

Robling, A. G., & Turner, C. H. (2009). Mechanical signaling for bone modeling and remodeling. *Crit Rev Eukaryot Gene Expr, 19*(4), 319-338. doi:10.1615/critreveukargeneexpr.v19.i4.50

Roforth, M. M., Fujita, K., McGregor, U. I., Kirmani, S., McCready, L. K., Peterson, J. M., . . . Khosla, S. (2014). Effects of age on bone mRNA levels of sclerostin and other genes relevant to bone metabolism in humans. *Bone, 59*, 1-6. doi:10.1016/j.bone.2013.10.019

Samsa, W. E., Vasanji, A., Midura, R. J., & Kondratov, R. V. (2016). Deficiency of circadian clock protein BMAL1 in mice results in a low bone mass phenotype. *Bone, 84*, 194-203. doi:10.1016/j.bone.2016.01.006

Sangoram, A. M., Saez, L., Antoch, M. P., Gekakis, N., Staknis, D., Whiteley, A., . . . Takahashi, J. S. (1998). Mammalian circadian autoregulatory loop: a timeless ortholog and mPer1 interact and negatively regulate CLOCK-BMAL1-induced transcription. *Neuron, 21*(5), 1101-1113. doi:10.1016/s0896-6273(00)80627-3

Santosh H Shankarnarayan, R. A., Amanda Hamilton, Dong L Barraclough, William D Fraser & Jiten P Vora. (2013). *Circadian rhythm of circulating sclerostin in healthy young men*. Paper presented at the 15th European Congress of Endocrinology, Copenhagen, Denmark.

Santosh HS, A. R., Hamilton A, Barraclough DL, Fraser WD, Vora JP. (2013). *Circadian rhythm of circulating sclerostin in healthy young men.* . Paper presented at the 15th European congress of endocrinology. , Copenhagen, Denmark.

Sato, T. K., Yamada, R. G., Ukai, H., Baggs, J. E., Miraglia, L. J., Kobayashi, T. J., . . . Hogenesch, J. B. (2006). Feedback repression is required for mammalian circadian clock function. *Nat Genet, 38*(3), 312-319. doi:10.1038/ng1745

Schilperoort, M., Bravenboer, N., Lim, J., Mletzko, K., Busse, B., van Ruijven, L., . . . Winter, E. M. (2020). Circadian disruption by shifting the light-dark cycle negatively affects bone health in mice. *FASEB J, 34*(1), 1052-1064. doi:10.1096/fj.201901929R

Schmid, B., Helfrich-Forster, C., & Yoshii, T. (2011). A new ImageJ plug-in "ActogramJ" for chronobiological analyses. *J Biol Rhythms, 26*(5), 464-467. doi:10.1177/0748730411414264

Schroeder, A. M., Truong, D., Loh, D. H., Jordan, M. C., Roos, K. P., & Colwell, C. S. (2012). Voluntary scheduled exercise alters diurnal rhythms of behaviour, physiology and gene expression in wild-type and vasoactive intestinal peptide-deficient mice. *J Physiol, 590*(23), 6213-6226. doi:10.1113/jphysiol.2012.233676

Skerry, T. M., Bitensky, L., Chayen, J., & Lanyon, L. E. (1989). Early strain-related changes in enzyme activity in osteocytes following bone loading in vivo. *J Bone Miner Res, 4*(5), 783-788. doi:10.1002/jbmr.5650040519

Srivastava, A. K., Bhattacharyya, S., Li, X., Mohan, S., & Baylink, D. J. (2001). Circadian and longitudinal variation of serum C-telopeptide, osteocalcin, and skeletal alkaline phosphatase in C3H/HeJ mice. *Bone, 29*(4), 361-367. doi:10.1016/s8756-3282(01)00581-6

Stern, A. R., Stern, M. M., Van Dyke, M. E., Jahn, K., Prideaux, M., & Bonewald, L. F. (2012). Isolation and culture of primary osteocytes from the long bones of skeletally mature and aged mice. *Biotechniques, 52*(6), 361-373. doi:10.2144/0000113876

Su, N., Yang, J., Xie, Y., Du, X., Chen, H., Zhou, H., & Chen, L. (2019). Bone function, dysfunction and its role in diseases including critical illness. *Int J Biol Sci, 15*(4), 776-787. doi:10.7150/ijbs.27063

Svedbom, A., Hernlund, E., Ivergard, M., Compston, J., Cooper, C., Stenmark, J., . . . IOF, E. U. R. P. o. (2013). Osteoporosis in the European Union: a compendium of country-specific reports. *Arch Osteoporos, 8*, 137. doi:10.1007/s11657-013-0137-0

Swanson, C., Shea, S. A., Wolfe, P., Markwardt, S., Cain, S. W., Munch, M., . . . Buxton, O. M. (2017). 24-hour profile of serum sclerostin and its association with bone biomarkers in men. *Osteoporos Int, 28*(11), 3205-3213. doi:10.1007/s00198-017-4162-5

Swanson, C. M., Kohrt, W. M., Buxton, O. M., Everson, C. A., Wright, K. P., Jr., Orwoll, E. S., & Shea, S. A. (2018). The importance of the circadian system & sleep for bone health. *Metabolism, 84*, 28-43. doi:10.1016/j.metabol.2017.12.002

Swanson, C. M., Shea, S. A., Wolfe, P., Cain, S. W., Munch, M., Vujovic, N., . . . Orwoll, E. S. (2017). Bone Turnover Markers After Sleep Restriction and Circadian Disruption: A Mechanism for Sleep-Related Bone Loss in Humans. *J Clin Endocrinol Metab, 102*(10), 3722-3730. doi:10.1210/jc.2017-01147

Tabatabaei-Malazy, O., Salari, P., Khashayar, P., & Larijani, B. (2017). New horizons in treatment of osteoporosis. *Daru, 25*(1), 2. doi:10.1186/s40199-017-0167-z

Takahashi, J. S., Hong, H. K., Ko, C. H., & McDearmon, E. L. (2008). The genetics of mammalian circadian order and disorder: implications for physiology and disease. *Nat Rev Genet, 9*(10), 764-775. doi:10.1038/nrg2430

Takarada, T., Xu, C., Ochi, H., Nakazato, R., Yamada, D., Nakamura, S., . . . Hinoi, E. (2017). Bone Resorption Is Regulated by Circadian Clock in Osteoblasts. *J Bone Miner Res, 32*(4), 872-881. doi:10.1002/jbmr.3053

Tu, X., Rhee, Y., Condon, K. W., Bivi, N., Allen, M. R., Dwyer, D., . . . Bellido, T. (2012). Sost downregulation and local Wnt signaling are required for the osteogenic response to mechanical loading. *Bone, 50*(1), 209-217. doi:10.1016/j.bone.2011.10.025

van der Spoel, E., Oei, N., Cachucho, R., Roelfsema, F., Berbee, J. F. P., Blauw, G. J., . . . van Heemst, D. (2019). The 24-hour serum profiles of bone markers in healthy older men and women. *Bone, 120*, 61-69. doi:10.1016/j.bone.2018.10.002

Wein, M. N. (2018). Parathyroid Hormone Signaling in Osteocytes. *JBMR Plus, 2*(1), 22-30. doi:10.1002/jbm4.10021

Willie, B. M., Birkhold, A. I., Razi, H., Thiele, T., Aido, M., Kruck, B., . . . Duda, G. N. (2013). Diminished response to in vivo mechanical loading in trabecular and not cortical bone in adulthood of female C57Bl/6 mice coincides with a reduction in deformation to load. *Bone, 55*(2), 335-346. doi:10.1016/j.bone.2013.04.023

Willie, B. M., Zimmermann, E. A., Vitienes, I., Main, R. P., & Komarova, S. V. (2020). Bone adaptation: Safety factors and load predictability in shaping skeletal form. *Bone, 131*, 115114. doi:10.1016/j.bone.2019.115114

Wolff, G., & Esser, K. A. (2012). Scheduled exercise phase shifts the circadian clock in skeletal muscle. *Med Sci Sports Exerc, 44*(9), 1663-1670. doi:10.1249/MSS.0b013e318255cf4c

Wolff, J. (1892). The law of bone transformation. *Berlin: Hirschwald*.

Xu, C., Ochi, H., Fukuda, T., Sato, S., Sunamura, S., Takarada, T., . . . Takeda, S. (2016). Circadian Clock Regulates Bone Resorption in Mice. *J Bone Miner Res, 31*(7), 1344-1355. doi:10.1002/jbmr.2803

Yamada, S., Saeki, S., Takahashi, I., Igarashi, K., Shinoda, H., & Mitani, H. (2002). Diurnal variation in the response of the mandible to orthopedic force. *J Dent Res, 81*(10), 711-715. doi:10.1177/154405910208101011

Yavropoulou, M. P., & Yovos, J. G. (2016). The molecular basis of bone mechanotransduction. *J Musculoskelet Neuronal Interact, 16*(3), 221-236. Retrieved from https://www.ncbi.nlm.nih.gov/pubmed/27609037

Yoo, S. H., Yamazaki, S., Lowrey, P. L., Shimomura, K., Ko, C. H., Buhr, E. D., . . . Takahashi, J. S. (2004). PERIOD2::LUCIFERASE real-time reporting of circadian dynamics reveals persistent circadian oscillations in mouse peripheral tissues. *Proc Natl Acad Sci U S A, 101*(15), 5339-5346. doi:10.1073/pnas.0308709101